AN ABSTRACT OF THE THESIS OF

Hannes Max Hapke for the degree of Master of Science in Electrical and Computer Engineering presented on June 8, 2009.

Title: Development of Biomimetic Control Strategies for the Optimal Use of Renewable Sources and Energy Storage Systems

Abstract approved: ____________________________________

Ted K.A. Brekken

In the year 2007, the worldwide energy consumption accumulated to a total of 16.5 billion MWh. While the resources of conventional energy production cause environmental damage, renewable energy sources like solar or wind power offer a solution to substitute for coal or nuclear generated power. Countries like Denmark and Spain have shown that a high penetration of renewable power is possible; however, the production shifts from a demand-driven production to a supply-driven electricity production. This causes the problem that energy could be available while the demand is low or vice versa. Energy storage could be a solution to this challenge.

This thesis investigates how an envisioned storage system for a wind park in northern Oregon could be controlled in order to optimize its capacity. Two biomimetic strategies, neural network and fuzzy logic control, were implemented and later optimized by a genetic algorithm to increase the profit from storing the electric energy in the storage unit.

Even though the optimization with genetic algorithms leads to improvements in the performance of the neural network and fuzzy logic controller, the results show that biomimetic controllers only perform as good as a simple, unconstrained power split controller. Both controllers are tested with several months of wind and price data.

Development of Biomimetic Control Strategies for the Optimal Use of Renewable Sources and Energy Storage Systems

by

Hannes Max Hapke

A THESIS

submitted to

Oregon State University

in partial fulfillment of
the requirements for the
degree of

Master of Science

Presented June 8, 2009
Commencement June 2010

Master of Science thesis of Hannes Max Hapke presented on June 8, 2009.

APPROVED:

Major Professor, representing Electrical and Computer Engineering

---

Director of the School of Electrical Engineering and Computer Science

---

Dean of the Graduate School

I understand that my thesis will become part of the permanent collection of Oregon State University libraries. My signature below authorizes release of my thesis to any reader upon request.

Hannes Max Hapke, Author

ACKNOWLEDGEMENTS

I would like to thank my advisers, Dr. Annette von Jouanne and Dr. Ted Brekken, for their support throughout my graduate studies. I am very grateful for their guidance during my thesis work and for the possibility of becoming a graduate student at the Wallace Energy Systems & Renewables Facility. Without the support of my advisers, the endeavor “Master’s abroad” would not have been possible.
I also want to express my gratitude to Dr. Zhaohui Wu and Dr. Karl Haapala for their endless help while working on my minor project. Because of their support, I was able to learn about a new field of environmental science (at least for me).
Furthermore, I also want to thank Dr. Mike Pavol for taking the time to be on my committee.
Mr. Mike Hulse from Bonneville Power Administration (BPA) and Mr. Chris Dieterle from Portland General Electric (PGE) deserve a big thanks for supporting my master’s thesis with real-life data. Funding and data support are greatly appreciated from BPA, Central Lincoln PUD, PGE, and PowerDex.
My thanks goes also to Zuan Yen, Chelsea Lalla, Kristin Glanville, Doug Halamay and all other graduate students at the WESRF lab. It was great working with you.

This thesis would not have been possible without the tremendous support of Dr. David and Deb Hackleman. I am very thankful for their support in making my graduate studies in the U.S. possible and for their wonderful friendship.

Most importantly, I want to thank my family for their support and encouragements. My partner, Joy, for all her support and love. My parents, Christina and Andreas, for their guidance and understanding for studying far away from home. My sister, Stefanie, for her encouragements during my graduate studies. And my grandparents and aunt for their support to study abroad.

TABLE OF CONTENTS

TABLE OF CONTENTS (Continued)

TABLE OF CONTENTS (Continued)

LIST OF FIGURES

LIST OF FIGURES (Continued)

LIST OF FIGURES (Continued)

LIST OF TABLES

Chapter 1 – Introduction

Energy is one of the most important commodities in the world. In the year 2007, worldwide energy consumption reached to a total of 16.5 Billion MWh [1]. This amount will raise with time due to the worldwide population, and gross domestic product increase, as well as due to the technological progression [2].

While the existing resources of conventional energy production cause environmental damage, renewable energy sources like solar or wind power offer a solution to substitute for coal or nuclear generated power. Countries like Denmark and Spain have shown that a production penetration of renewable power is possible. With this high percentage of wind power penetration (above 20%), the production shifts from a demand-driven production to a supply-driven electricity production [3]. When only fuel-based generation like coal or nuclear power is used, the production is adjusted to the demand. In a supply-driven production, the goal is to harvest as much energy as possible. This causes the problem in which energy could be available while the demand is low or vice versa. Energy storage could be a solution to this challenge. However, the investment costs for energy storage systems are high. Nevertheless, in an April 2009 report by the North American Electric Reliability Corporation (NERC), the organization recommends energy storage as one possibility to help integrate wind power into the grid [4].

The existing literature [5, 6, 7] showed clearly that two philosophies about energy storage exist, which are highly connected to the structure of the electric grid. If the grid is dense and well interconnected between regions with different natural sources (like wind, solar, hydro), then fluctuations of one energy source can be balanced out by another source from a different region [6]. In Europe, excess wind energy from Denmark or Germany can be stored as pumped hydro power in Norway or Austria.

If the grid is spread out over a large service area and the transmission capacity is limited, like in the U.S., then a local storage of the energy in batteries, flywheels, etc. is preferable citeMcdowall2005. In this case, energy does not need to be transported over large distances, but the capacity is limited to the maximum of the storage system. Depending on the energy storage system, the saved energy can be used to support stability, load following, peak reduction or even seasonal storage (see Figure 1.1).

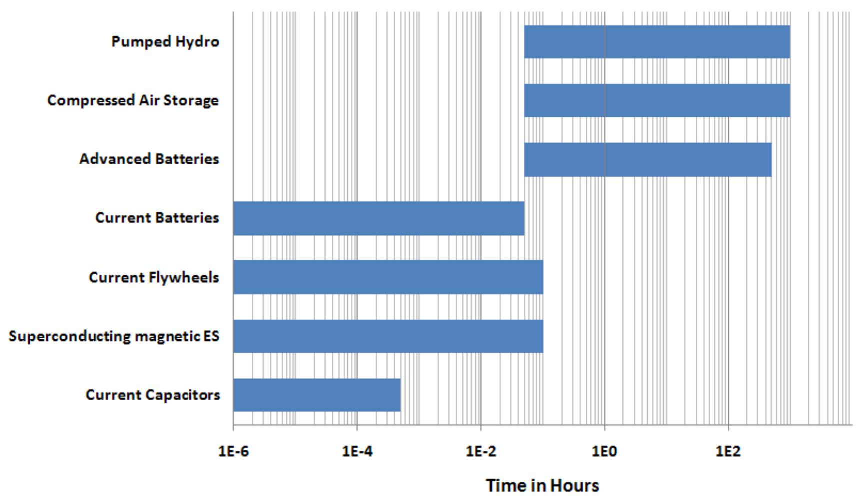

Figure 1.1: Overview of Energy Storage Technologies and theirs Characteristic Times [8]

1.1 Energy Storage Technologies

Supercapacitors Supercapacitors are mainly used to level out power quality fluctuations within a time frame between a few seconds and minutes [9]. The energy is stored as electrostatic energy [8]. Because of the low market penetration, supercapacitors are extremely expensive; current prices range from $25,000/kWh up to $45,000/kWh [9].

Superconducting Magnetic Energy Storage According to the Sandia Report on energy storage [9], Superconducting Magnetic Energy Storage (SMES) could be used for various time frames [9], but is currently only produced for power quality purposes. The energy is stored as electromagnetic energy in superconducting magnets, which need to be cooled down to extreme low temperatures. The efficiency of SMES systems is extremely good (around 95%), but the installation costs are also very high (around $50,000/kWh) [9].

Flywheels Flywheels store the excess energy as kinetic energy [8]. Flywheels also show a high efficiency with a low maintenance rate [9]. For a 50kWh system, costs are estimated to be around $1000/kWh [9].

Zinc/Bromine Batteries Zn/Br batteries are flow batteries, in which electrodes are separated from energy storage liquid. If the battery is charged, zinc is plated on the electrode and vice versa [9]. According to the Sandia Report, Zn/Br batteries are well suited for long-term energy storage [9]. The costs are estimated to be around $400/kWh for a 50kWh unit.

Compressed Air Energy Storage The idea behind compressed air energy storage is to use the excess energy to pressurize an underground reservoir with air. If energy is needed, then it would be released [8]. A few systems were constructed, for example in Huntorf, Germany [9]. The energy can be stored for a long time frame.

Pumped Hydropower Another energy storage option for long-term storage is pumped hydropower. Hereby, the excess renewable energy is used to pump water to a higher location and thus store the energy as potential energy [8]. Various sites with pumped hydropower exist throughout the world. The construction costs are very expensive ($1000/kW), but the capacity costs are inexpensive (around $10/kWh) [9].

1.2 Idea of this Thesis

Energy storage systems are capital intensive, which often jeopardizes their benefit. It is estimated that an envisioned battery system for a wind park in northern Oregon costs up to 30% of initial investment and could increase the electricity production costs by almost a third (see Section 3).

Since the energy density of batteries, flywheels, etc. is relatively low, a load following to balance out times with no wind is hardly feasible. Therefore, the energy storage system for a wind park is supposed to balance out fluctuations between a wind power forecast, which was generated one hour prior, and the actual, current production. However, an energy storage system can also serve another purpose. Since the market price fluctuates over the course of a day, week or month, (see Figure 3.1) and the stored energy is limited, the core idea of this thesis is to develop control strategies to increase the revenue from storing energy in the storage system. Energy could be held back if the price, and therefore the penalty for incorrect forecasts, is low. In case the price rises in the near future, energy could also be kept back and sold later at a higher price.

It was envisioned that a controller, as shown in Figure 1.2, between the wind park, the energy storage system, and the electric grid controls the optimal power flow. Furthermore, the controller was designed to generate a discrete output command based on four input variables (Figure 1.3):

- Battery State-of-Charge
- Power Difference between the current Power Production and the Power Forecast
- Current Price Indicator
- Future Price Indicator

The output command can be: Store, sell, and hold. If energy should be stored for a later time, the command "store" is preferred. The command "sell" allows to offset an energy deficit. The third command "hold" prevents an interference of the controller with the power flow between the wind park and the grid.

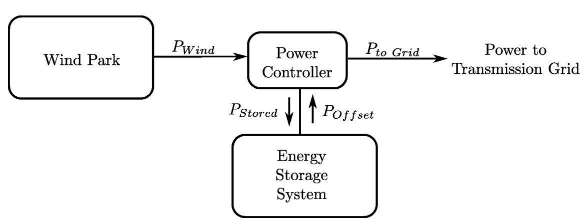

Figure 1.2: Power Flow between the Wind Park, the Energy Storage System and the Power Grid

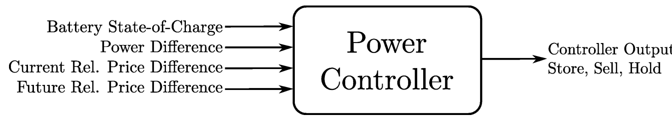

Figure 1.3: Generic Power Controller with Inputs and Outputs

1.3 Biomimetic Control

It is difficult to determine the optimal solution for the stated storage problem depending on the four input parameters solely based on expert knowledge. Therefore, the hypothesis of this work is that a control system that determines its behavior by itself performs better than a simple power controller.

Biomimetic control strategies have a history in the field of energy systems. As Kalogirou [10] and Warwick [11] point out in their publications, neural networks and fuzzy logic controllers were used for problems like fault detections [11], control of solar panels [10], wind power predictions [10], etc. The benefit of biomimetic control approaches are that they adapt to unknown situations and can find a near-optimal solution for a given problem [11].

1.4 Literature Review

Biomimetic control strategies for wind power integration have been presented in a few papers. Yan et al. [12] published a method based on fuzzy control to optimize the wind power integration into the grid. They stated that the wind power generation, system demand, spinning reserves, etc. are afflicted with uncertainties; Therefore, the best method to control these uncertainties is a fuzzy controller.

Jurado et al. [13] presented a neuro-fuzzy controller for a wind-diesel system. The controller's goal was to find the optimal balance between the renewable energy power and diesel-generated power for the automatic voltage control.

An application of a modern control technique for energy storage systems was published by Panickar et al [14]. In the publication, the research group of the Curtin University of Technology presented a "neuro-fuzzy model" that optimizes the load dispatch. However, the solution did not consider the economic aspect of storing the excess energy.

An economic dispatch model based on fuzzy logic was presented by Attaviriyanupap et al. [15]. The presented approach optimizes the scheduling of renewable sources. Miranda et al. [16] presented a similar method, also based on fuzzy logic, to optimize the dispatch between conventional and renewable energy sources. However, both publications do not consider the aspect of energy storage. Therefore, it became interesting to implement a biomimetic control approach to optimize the use of an energy storage system with a focus on the economic aspect.

1.5 Outlook

This thesis will be split into six chapters. First, Chapter 2 will give an introduction into biomimetic control techniques. It will introduce neural networks, fuzzy logic controllers and the optimization technique of genetic algorithms. Chapter 3 will present the basics of the economics of energy production. It will explain how electricity is traded, how this influences the price, which price indicator was selected for this thesis, and will introduce the cost function for the optimization. An introduction to the life cycle assessment of wind parks is presented in chapter 4. The goal of that chapter, which was done as a minor project, was to determine the environmental impact of renewable energy technologies, in terms of savings throughout their lifetime.

Following the theoretical discussion, the implementation of neural network and fuzzy logic controllers and their optimization is explained in chapter 5. The results of this analysis will be presented in chapter 6, ending with conclusions and the outlook for possible future work.

Chapter 2 – Theoretical Background on Biomimetic Control and Optimization Techniques

Biomimetic techniques have a long history in controls. For a long time, researchers tried to imitate nature's clever techniques to adapt, optimize, and control. In 1943, psychologist, McCulloch, and MIT professor, Pitts, proposed the theoretical idea of an artificial neuron [17]. Based on this fundamental publication, various network types were developed. In 1965, former UC Berkeley professor, Lotfi A. Zadeh, introduced fuzzy logic [18], which became the fundamental idea of fuzzy control in following years. Around the same time, various researchers developed the idea of simulated evolution used for optimizations. One of the early founders was British geneticist, Alex Fraser, who published his ideas in 1957 [19]. All developments had in common the idea of mimicking nature's successes. Today, the theory of neural networks and fuzzy logic are widely used for "decision-making" processes in the field of control theory, and genetic algorithms became an accepted approach for the optimization of systems.

This chapter will briefly introduce the concepts of neural networks, fuzzy controllers and genetic algorithms for a better understanding of the proposed controller solution. First, a short literature review of applied biomimetic control techniques in power systems in presented. Later, the chapter introduces neural networks and fuzzy logic, presents a brief comparison between the two techniques and concludes with an explanation of genetic algorithms.

Recommended Literature Since the presentation of the biomimetic techniques will be brief, the reader is pointed to further literature for a broader introduction. A good introduction into "Neural Networks" was written by Raúl Rojas [17], a computer science professor at the Free University of Berlin, Germany. Kevin Passion from the Ohio State University published an introduction to "Biomimicry" in 2004 [20]. The book introduces neural networks, fuzzy logic and genetic algorithms. "Systems and Control" by Stanislaw Zak [21] demonstrates how biomimic techniques can be used in modern control theory. Zak also emphasizes how genetic algorithms can be used to optimize fuzzy sets.

2.1 Applications in Power Systems

For over 15 years, biomimetic approaches have been applied in power systems research. Whether used for fault detecting or voltage control, neural networks show good performance [11]. Today, genetic algorithms are used in the design of complex systems, the generator design [22]. Furthermore, biomimetic techniques have been widely applied in the field of renewable energy research, whether for wind power predictions, reactive power control, or for the optimization of solar plants [10].

2.2 Introduction in Neural Networks

The field of neural networks is expansive. It ranges from the early proposed idea of a single neuron, suggested by McCulloch and Pitts, to multi-layer networks [17]. All neural networks have at least one thing in common; They are based upon one or more single neurons, which are "simple nonlinear elements" [11]. This section will introduce the basic ideas of neural networks and explain the main terminology for a better understanding of the later presented solution.

2.2.1 Applications of Neural Networks

According to Kalogirou et al. [10], neural networks are “good for some tasks while not so effective in some others”. Neural networks can be seen as a statistical tool [23], which maps input to output values and approximates the underlying function. They are useful to apply to incomplete or noisy data sets and their behavior is “robust and fault tolerant” [10].

The main applications for the networks are:

- Function approximation
- Pattern recognition
- Associative memory
- Generation of meaningful patterns

Because of the last main application, neural networks are well-suited for a decision-making controller, especially for the power flow control of a storage controller.

2.2.2 A Single Neuron

It was always humans’ wish to program computers in a manner, which “would mimic the organization of the brain” [21]. However, the human brain is one of the most complex systems in nature, so McCullon and Pitts began by modeling a single neuron [17]. In nature, one neuron is connected to its neighbor neurons, and small electric signals are transmitted from one neuron to the next. Depending on the excitation from other neurons, a neuron may create an electric output signal [21]. According to Zak, observations in nature revealed that single neurons only create an output signal if their "stimuli" exceed a certain threshold, and they received multiple inputs from different neighbor neurons [21].

This is the fundamental idea of a theoretical single neuron, which represents a threshold unit that can be activated depending on the "stimuli".

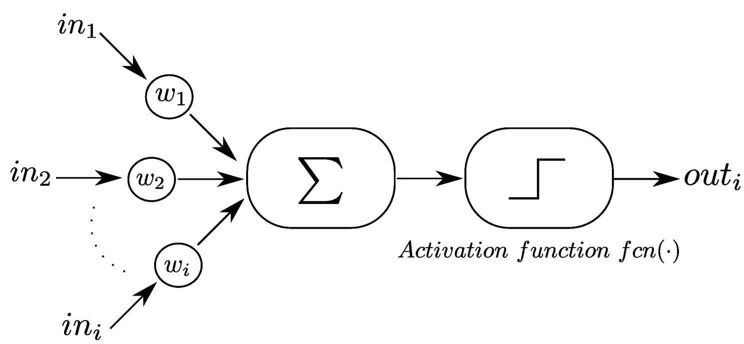

Figure 2.1: Structure of a Single Neuron

Figure 2.1 shows that all input signals from other neurons are weighted, internally summated and passed on to an activation function. Mathematically, this can be represented as follows:

$$out_i = fcn\left[\sum_{k=1}^{n} in_{ki} \times w_{ki} + w_0\right] \tag{2.1}$$

in_{ki} are the input signals from the neighbor neurons. w_{ki} determines how the input signals are weighted at time step t and w_0 is the bias of the particular neuron. The input to the bias weight is always one. According to Rojas [17], a bias is helpful to speed up the learning process.

$fcn(\cdot)$ represents the activation function of the neuron. Generally, the output of the activation function is supposed to be one if the sum of all weighted inputs is above a threshold S. Otherwise the output is supposed to be zero [23].

$$fcn\left[\sum_{k=1}^{n} in_{ki} \times w_{ki} + w_0\right] = \begin{cases} 1, & if\ \sum in_{ki} \times w_{ki} + w_0 > S \\ 0, & otherwise \end{cases} \tag{2.2}$$

However, for the training purpose of the neural network, it is important that the activation function is fully differentiable (see 2.2.4). Therefore, the linear, the sigmoid or the hyperbolic tangent function (shown in Equation 2.3, 2.4 and 2.5, as well in Figure 2.2) became popular to use as an activation function, because of the simple computable derivative (this is very practical for the learning process, as shown in Section 2.2.4) [23].

$$linear(x) = cx \tag{2.3}$$

$$sigmoid(x) = \frac{1}{1+e^{-x}} \tag{2.4}$$

$$\tanh(x) = \frac{e^{2x}-1}{e^{2x}+1} \tag{2.5}$$

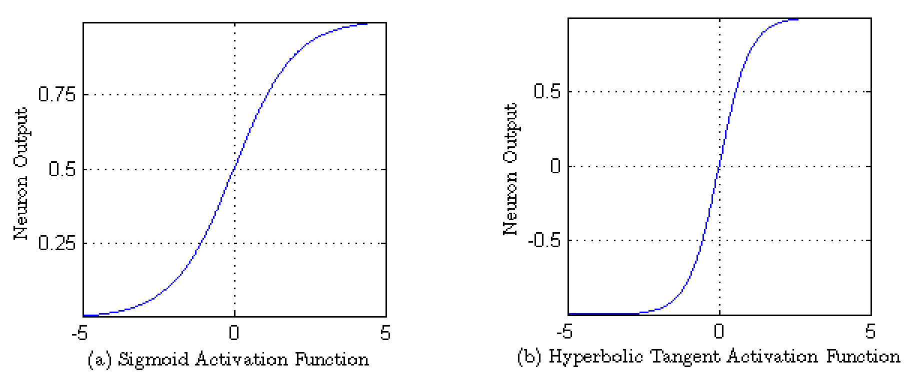

Figure 2.2: Sigmoid and Hyperbolic Tangent Activation Functions

2.2.3 Network Architectures

After McCullon and Pitts' initial idea of a single neuron, different network architectures evolved. The number of problems that can be solved by a single threshold unit is fairly small. Thus, the following network types, as seen in Figure 2.3, evolved to represent the learned knowledge.

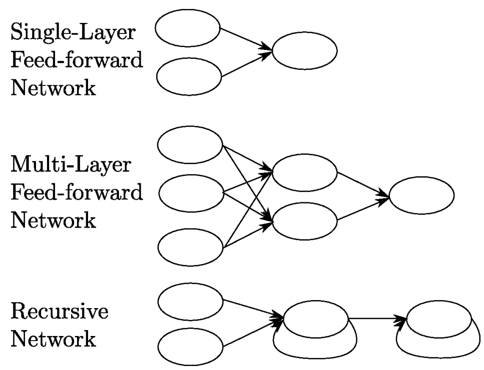

Figure 2.3: Different Neural Network Architectures

The multi-layer feed-forward network type is the most used architecture today and the presented neural network in this thesis uses a multi-layer architecture.

2.2.4 Backpropagation Algorithm

It is now of interest to adjust the weights w between the input and output layer in such a way that the network finds, for every presented input, a solution with the smallest error. A way to "train" the neural network is the backpropagation algorithm. The algorithm calculates, in a "forward pass", the activation function outputs for every neuron and compares the final result of the output layer y with a presented training example d. In the "backward pass", the weights between the neurons are adjusted "in order to reduce the learning error" [21]. Figure 2.4 shows the structure of the developed neural network with its three layers: input, hidden, and output layer.

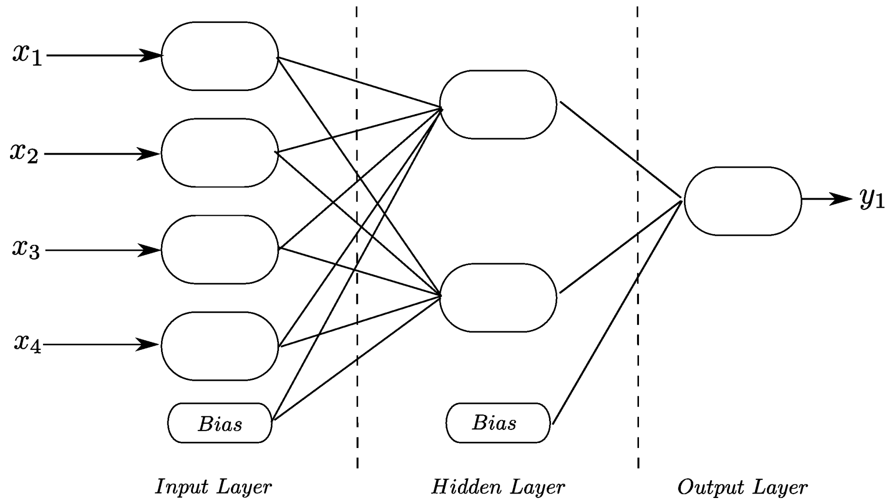

Figure 2.4: Multi-Layer Neural Network Structure

The error of the output layer is defined as:

$$E = \frac{1}{2}\sum_{j=1}^{k}(d_j - y_j)^2 \tag{2.6}$$

In general, the change in error as a function of the change in each weight can be described by

$$\frac{\partial E}{\partial w_{ij}} = e_j \frac{\partial e_j}{\partial w_{ij}} \tag{2.7}$$

$$= -e_j \frac{\partial fcn(\cdot)_j}{\partial w_{ij}} \tag{2.8}$$

where e is the difference between the desired output d_j and the calculated output y_j.

Here, the property of simple activation function differentiability is useful since the derivative of the hyperbolic tangent function is

$$\frac{\partial \tanh(x)}{\partial x} = 1 - \tanh(x)^2 \tag{2.9}$$

and for the sigmoid function $sigmoid(x)$

$$\frac{\partial sigmoid(x)}{\partial x} = sigmoid(x)(1 - sigmoid(x)) \tag{2.10}$$

The final change of the individual weight during the "backward pass" is given by η times the error change and can be seen in Equation 2.11. η is the "learning rate" of the network and determines how fast weight values get adjusted.

$$\Delta w_{ij} = -\eta \frac{\partial E}{\partial w_{ij}} = \eta \delta_j x_i \tag{2.11}$$

with

$$\delta_j = \begin{cases} fcn'(\cdot)(d_j - y_j) & \text{for the output layer} \\ fcn'(\cdot)\sum_k \delta_k w_{jk} & \text{for the hidden layer} \end{cases} \tag{2.12}$$

This learning rule is called gradient descent because it updates the weights according to the steepest change, the gradient. It is important to mention that for the error calculation of one neuron, the error of the neurons in the previous layers have to be known. Thus, this step is called the "backward pass", since it goes backwards layer by layer.

The weights are finally updated by

$$w_{ij}^{t+1} = w_{ij}^{t} + \Delta w_{ij} \tag{2.13}$$

Once the weights are updated, a new training set is presented to the neural network to continue with the training.

2.2.4.1 Implementation of Backprogation

Table 2.1 summaries all steps of a backpropagation implementation. Starting off with random weight values for each neuron connection, over the time of several iterations, the weights will be adapted to the training sets and a solution with a minimal error will established. Once the training stops, either by termination due to a maximum number of iterations or due to a minimal error, the established connection weights can be saved and used for the later application of the network.

Table 2.1: Implementation of the Backpropagation Algorithm

PSEUDOCODE Backpropagation Implementation
Step 1 Load training set $(x_1, d_1, \ldots, x_n, d_n)$
Step 2 Initialize all weights to random values from the interval $\pm 0.5/\sqrt(n)$; where n is the number of neurons in the layer of the weight
Step 3 Calculate the forward-pass of the neural network
Step 4 Calculate the error between the desired and calculated output
Step 5 Propagate the error back through the layers during the backward-pass. Adapt the weights according to the error gradient.
Step 6 If the last error is below a minimum training error or if the maximum number of iterations is reached, stop the training; otherwise return to Step 1

This derivation of the backpropagation algorithm was brief and a few steps were neglected. For more and detailed information on the derivation, the reader is pointed again to the publication by Rojas [17], who also introduced a very short matrix implementation of the backpropagation algorithm.

2.2.5 Details on Neural Networks

Multiple details can be important when a neural network is trained. Attention should be paid to how training subsets are selected when they are presented to the neural network input layer. Another important fact can be the chosen architecture of the neural network. As an example, should neurons have an recursive input (as presented in Figure 2.3)? The following sections address the most important details for the implementation of this thesis.

2.2.5.1 Supervised vs. Unsupervised Training

The training of a neural network, basically the adjustment of the weights, can be done in two ways. If information about the desired controller output are available prior to the training, then a supervised training is possible and preferred. Supervised training means that the forward-pass is calculated, the error is determined, and the weights are changed according to the error. Essentially, the entire backpropagation algorithm is performed. In this case, the weights are adjusted directly from the output error, and performance of the network can be assessed without broader system interactions (shown in Figure 2.5).

If training data for a desired output are not available, such as the case of an unknown behavior of the system, then the training of the network needs to be done unsupervised. Here, the performance of the network is evaluated according to the performance of the broader system, which is controlled by the neural network. In this case, only the forward pass of the network is calculated, and the output value is passed on to the outside system.

Then, the system's action due to the network output is evaluated and the network weights are changed according to the performance, for example, through a genetic algorithm (shown in Figure 2.5).

2.2.5.2 Online vs. Offline Training

A training of a neural network is called offline if the weights of the network are adjusted before the network operates in real life. In contrast, during an online training, the weights of the network can be changed during the operation. The advantage of an offline training is that the final solution can be investigated for singularities prioir to the operaion of the network. During an online training, the weights can be changed during the operations, and the calculated solution might not be applicable.

2.2.5.3 Learning Rate

An important detail in neural networks is the learning rate η. This value, usually between 0 and 1 (Duda et al. [24] recommends a learning rate around 0.1), determines how much the error will affect the rate of weight change. η has a strong influence on how fast a

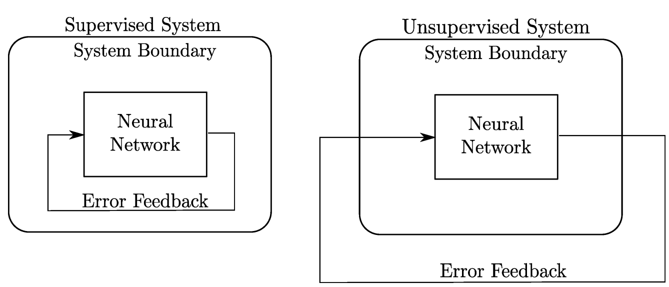

Figure 2.5: Difference of the Error Feedback for Supervised and Unsupervised Systems

problem is learned. If the optimal η is found, the training for an optimal solution can be done within one training step [24]. Figure 2.6 shows how η can influence the training of a weight. If the learning rate is below the optimal learning rate then the weight gradually approach the optimal weight. In contrast, if *eta* is above the optimal learning rate, the weight will oscillate around the optimal weight.

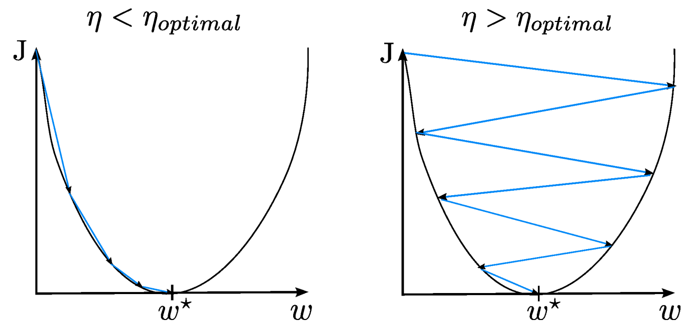

Figure 2.6: Influence of η on the Learning Performance

2.2.5.4 Generalization

If a data set is available for the training of a neural network, all data are usually not used for the training of the network. The data are typically split into three sets: training data, validation data and generalization data. The training data, the majority of the data set, are used to train the network, as described earlier. The validation set is used to confirm that the learning rate was chosen well and that the network performs well even for the cases for which it was not trained. The generalization of the network, based on the generalization data, checks the overall performance of the entire network and verifies its function [24].

2.3 Introduction in Fuzzy Logic

As shown in the previous section, neural networks obtain their knowledge for decision-making through training and adjustment of the neuron weights. Another approach to obtain control decisions is fuzzy logic.

The uncertainty of the optimal decision makes it difficult to use traditional logic, so-called crisp logic. However, fuzzy logic tries to incorporate the "imprecision of the human-reasoning by representing uncertainty for the input variables" [11]. An input variable is represented by a set of values, which is called the membership function. For each input value, a "degree of membership" is calculated. With the results of this step, the fuzzy logic can be applied and the output result for a specific, predefined fuzzy rule, can be computed.

A key element in fuzzy logic is linguistic variables. The entire input space can be split up into regions, such as low, medium or high. Based on the linguistic variables, controller rules can be defined in plain verbal language, e.g. "IF Temperature is Low and Daytime is Morning THEN turn Furnace On".

Often nature works in a similar way. For example, light hits the eyes' retina and, according the wavelength, a photo receptor in the receptor cell creates an electronic impulse, which is then sent off to the brain.

The next sections will explain the background of fuzzy logic in more detail.

2.3.1 Fuzzy Set Theory

When Professor Lotfi A. Zadeh introduced the idea of fuzzy sets in 1965 [18], he laid out the basis for the fuzzy controller. The main idea was the linguistic description of logic relationships and the representation of the uncertainty of the logic variables. The next three sections lay out the main important basics: Linguistic Variable, Fuzzy Set, and Membership and Fuzzy Logic.

2.3.1.1 Linguistic Variable

The main idea of linguistic variables is to divide the input range of the variables into regions, which can be described by words. As mentioned earlier, the input range of variable *temperature* could be described by *low*, *medium* or *high*. There is no limit on fineness. The input range could be divided into a large number of sections. However, the entire input range must be covered. The choice of the linguistic variables has no "influence on the operation of the fuzzy controller" [20]; it helps to construct the rules later.

2.3.1.2 Fuzzy Set and Membership

In crisp sets, a variable may be part of the set or not. The result could be easily represented by a true/false statement. However, input variables are often afflicted with uncertainty (for example, through sensor errors). In this case, traditional logic is not preferable.

Contrary to crisp logic, fuzzy logic determines the "degree of membership", also called the "degree of truth" [11]. The "degree of membership" is determined by the membership function $\mu(x)$, which can be represented by various functions, as shown in Figure 2.7. Figure 2.8 shows an example how membership functions can cover the entire range of an input variable.

2.3.1.3 Fuzzy Logic

Crisp logic makes it simple to compute logical conjunctions like AND, OR, or NOT. The computation of fuzzy logic is not more difficult, but needs further definition.
In fuzzy logic, a union between two fuzzy memberships can be described by

$$\mu(a)\ AND\ \mu(b) = min\{\mu(a), \mu(b)\} \tag{2.14}$$

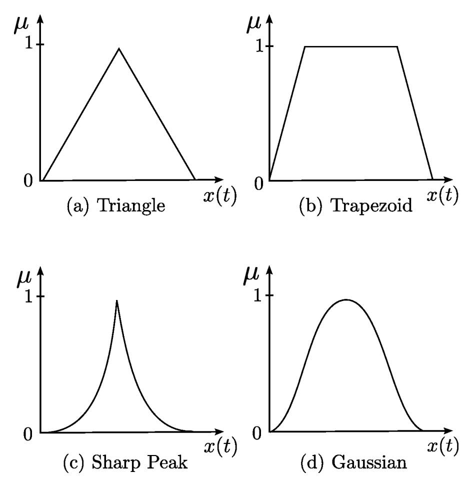

Figure 2.7: Examples for Membership Functions [20]

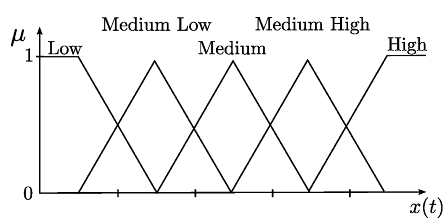

Figure 2.8: Example for a Set of Fuzzy Membership Functions

where the lower of the two values is always the result of the union. The intersection of two variables can be computed in fuzzy logic by

$$\mu(a)\ OR\ \mu(b) = max\{\mu(a), \mu(b)\} \tag{2.15}$$

The fuzzy complement is always given by

$$NOT\ \mu(a) = 1 - \mu(a) \tag{2.16}$$

2.3.2 Fuzzy Logic Controller

A fuzzy logic controller is based on the previous explained principles of the fuzzy logic. To make a decision, a fuzzy controller consists for four internal steps [10]:

- Pre-Calculation Procedures
- Fuzzification
- Takagi-Sugeno Inference
- Defuzzification

Each step is explained in the following sections.

2.3.2.1 Pre-Calculation Procedures

Before the fuzzy controller comes into place, the membership functions have to be defined for all input variables and their input ranges. In addition, all fuzzy controller rules have to be determined. Here, the concept of linguistic variables is very helpful, because the rules can be easily described and transformed into mathematical terms. For example, the statement

> IF SOC is High AND IF Power Difference is High Positive THEN Power Output is High Positive

stated mathematically by

$$y(a, b, k) = min(\mu_{SOC\ High}(a), \mu_{Power\ Difference\ High}(b)) \times k \tag{2.17}$$

where a and b are the sensor values for the battery capacity and the power difference, respectively, μ is the membership function for the particular linguistic variable, k is the constant output of the controller for this particular rule and $y(a, b, k)$ is the value of truth for this rule.
Once these membership functions and controller rules are determined, the actual controller process can begin.

2.3.2.2 Fuzzification

The first step of the fuzzy controller is the fuzzification. During this step, the degree of membership for every input variable and membership is determined. Figure 2.9 shows an example:

For the input value of $x = 0.2$, the degree of truth for every membership function is

$$\begin{aligned} \mu_{Low} &= 0.9 \\ \mu_{Medium} &= 0.1 \\ \mu_{High} &= 0 \end{aligned}$$

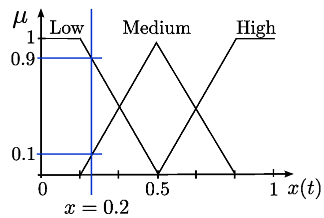

Figure 2.9: Example of the Fuzzification of the Input Variable x

The shown calculation is done for all input variables, and passed on to the Takagi-Sugeno inference method.

2.3.2.3 Takagi-Sugeno Inference Method

Kalogirou et al. [10], called the "inference mechanism, the heart of a fuzzy system". During this step the logic statements are evalutuated. The translated fuzzy rules (like in the example of Equation 2.17) determine the "truth value" of each output calculation. The inference method used in this thesis was first presented by the scientist Sugeno in 1985 [10], in which the output of a rule is a constant k (some value, which can represent an actual controller output value). This constant k is later weighted by the truth value, which is equivalent to the results of the membership functions.

2.3.2.4 Defuzzification

The last step of a fuzzy controller is the defuzzification, in which the computed outputs are weighted by their membership functions and aggregated to determine the overall output of the controller:

$$c = \frac{\sum_i k_i \times y_i}{\sum_i y_i} \tag{2.18}$$

k_i is the output value for the ith rule, whereas y_i is the weight of the ith rule and c is the overall output for the controller at the time step t. The result of Equation 2.18 can ultimately be applied to the outside world.

2.3.3 Implementation of a Fuzzy Controller

Table 2.2 shows the implementation steps for a fuzzy controller and summarizes all the steps, which were presented earlier.

Table 2.2: Implementation of the Fuzzy Controller

PSEUDOCODE Fuzzy Controller Implementation
Step 1 Initialization of the membership functions
Step 2 Fuzzify crisp input variables and determine the degree of membership during the fuzzification step
Step 3 Apply the fuzzification rules and compute their inference with the Takagi-Sugeno method
Step 4 Defuzzify the controller output by weighting each rule output
Step 5 Return to Step 2 for the next time step

2.4 Comparison of a Neural Network with Fuzzy Control

Neural networks and fuzzy logic are both methods to determine a controller decision. The main difference between these two concepts is the fact that “neural networks obtain their knowledge through training" [11], whereas the fuzzy system relies on a set of predefined rules [11]. A neural network can be trained by the actual data and determine the relationship between the inputs by itself, whereas the rules for a fuzzy controller rely on human interpretation of the data. However, reasonable training parameters have to be set for the neural network training. Otherwise, the training will be unsuccessful. An advantage of a fuzzy controller is the traceability of a solution. In contrast, in a neural network, the output relies on random weight values, which can be hard to trace for every time step.

2.5 Optimization Strategies

For various problems, it is often of interest to optimize a solution to reach a global minimum or maximum. If the given problem is simple enough, an analytical solution, such as through a derivation, is the best approach for optimization. However, if the problem is complex or the internal transfer function is unknown, sophisticated search algorithms are needed to find the global and best solution.
Generally, their are two approaches for search algorithms:

- Single Solution Search
- Population-based Search

Single solution search approaches always generate only one solution per iteration. A popular representative of this approach is "simulated annealing", in which a new solution is generated each iteration through slight variations of the previous solution, and the new solution is accepted with a probability that becomes smaller over time (thus originates the name of the algorithm). However, single solution approaches are not further discussed in this thesis and the reader is pointed to a publication of Richard Duda [24], which explains stochastic searches in detail.

In this work, the main focus will be on the population-based search approach, especially, genetic algorithms. This optimization idea, borrowed from nature to create new solutions, was "inspired by biological genetics" [21].

2.5.1 Genetic Algorithms

The central concept of genetic algorithms is that new solutions can be found by genetic manipulations like cross-over, mutation, or selection of previous solutions. The algorithm is designed so that solutions with good fitness will be the basis for further manipulations. If a solution is poor, then it gets discarded. Since the idea of genetic algorithms was adopted from biology, a lot of terms from that field are used to describe the algorithm. For example, a solution can be represented by a vector of neural network weights, and this solution is then called a chromosome. During each iteration, which is called an epoch, a pool of chromosomes is created through cross-over and mutation based on their parent chromosomes. Each chromosome is then evaluated and the fitness is determined. A fixed number of the chromosomes with the best fitness become the next parent chromosomes for the following epoch.

The following section explains the two most important concepts of chromosome manipulation: cross-over and mutation. Further manipulations are selection, in which a group of chromosomes are selected according to a criteria, elitism, in which chromosomes with the best fitness are taken for the new parent chromosomes [22], and replication, in which a chromosome with a good performance is copied to enhance its chance of replication.

2.5.1.1 Gene Manipulations

Cross-over Operation During the cross-over operation, two chromosomes are randomly selected from the chromosome pool and both are split at a random point. The remaining parts of the parent chromosomes X and Y create the new child chromosome (as shown in Figure 2.10).

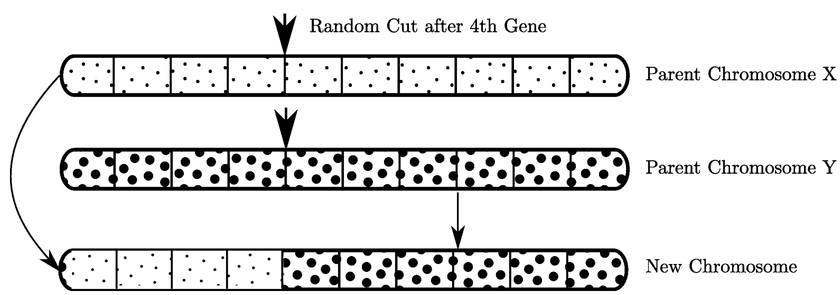

Figure 2.10: Example for One-point Crossover

Mutation The mutation operation selects a chromosome out of the chromosome pool with probability $P_{Selection}$ and manipulates a random number of genes within the chromosome. Each entry is then replaced by a new value, as Figure 2.11 shows.

2.5.1.2 Optimization of Neural Networks

Genetic algorithms can be used to optimize neural network weights, which were trained before. Here, the idea is that the set of weights is represented in one chromosome and

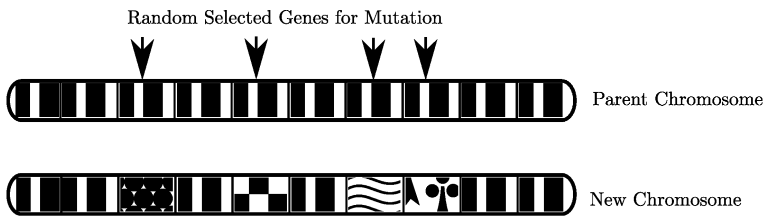

Figure 2.11: Example for Mutation of a Chromosome

the weighting solution is fine-tuned through various chromosome generations. Figure 2.12 shows an example of a chromosome that is generated from the network weights.

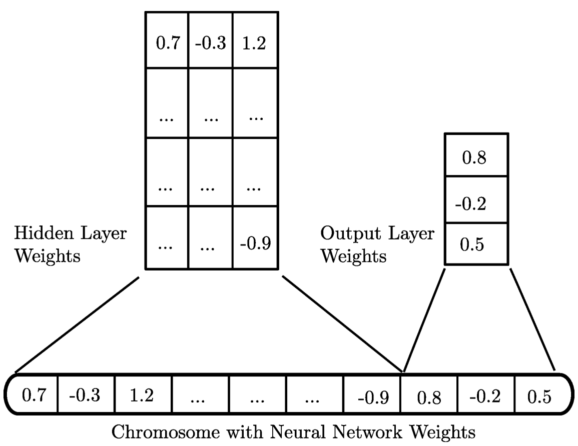

Figure 2.12: Example for Distribution of Network Weights in a Chromosome

During each epoch, new chromosomes are generated through gene manipulation and their fitness is evaluated. The best set of weights after a fixed amount of iterations is the final solution set for a neural network.

2.5.1.3 Optimization of Fuzzy Controller

Genetic algorithms can optimize a fuzzy logic controller in two ways:

Genetic algorithm adjusts the fuzzy membership rules: The set of different fuzzy rules can be described by a look-up table with n-dimensions (where n is the number of inputs). Each controller output is numbered and the look-up table references the number of the desired output. A chromosome contains the sequence of output rule numbers. The genetic algorithm manipulates these entries and adjusts the different fuzzy rules [21]. This approach was not pursued in this thesis due to the limited number of output solutions for the given problem.

Genetic algorithm adjusts the fuzzy membership functions: Another possibility of using genetic algorithms to optimize a fuzzy controller is to tune the membership functions. In this case, each entry of the chromosome represents the peak points of each membership function. For simplicity, each peak point is also the low point of the neighboring membership function (shown in Figure 2.13). For easier calculation, Zak et al. [21] suggest that the membership functions are centered around zero so that they are symmetrical to zero. The benefit of this idea is that the entire solution space is covered and no functions overlap when they are both at their peak. It also reduces the number of chromosome entries.

2.6 Summary

This chapter introduced three main representatives of biomimetic control. Neural networks were introduced and the training algorithm "backpropagation" was explained. It

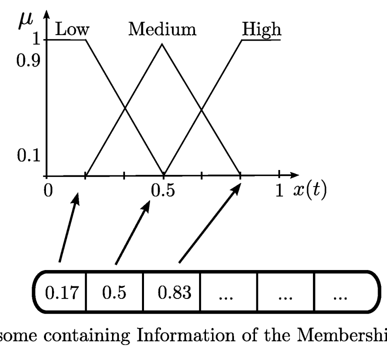

Figure 2.13: Example how a Genetic Algorithm adjusts the the Membership Functions

was shown that neural networks obtain their knowledge through learning of training patterns. In addition, a fuzzy controller with its fuzzy logic was presented. It was shown that input variables can be fuzzified and, in contrast to crisp sets, they can be partial members of a set. The importance of fuzzy logic was described, through which the knowledge of the fuzzy controller can be described. Lastly, genetic algorithms were introduced as a possible means of optimizing the solutions from fuzzy and neural network controllers. Based on evolutionary principles, previous solutions can mutate, cross-over, or not be selected as part of a process of generating new, better solutions. All three examples adopt strategies from nature for their operation and can be applied to power system problems.

Chapter 3 – The Economics of Energy

It is essential to know the basics of energy economics to understand the optimization process of the algorithm presented later. Since it is a huge field of study, in the following sections, only fundamental information is presented at a basic level.

This chapter introduces the concepts of electricity pricing, balance costs and, the costs of wind power. At the end of this chapter, different forecasting methods for price predictions are introduced and compared. Finally, the compositions of the cost functions used in this thesis are presented. These comprise the most important results from this chapter, because all optimization approaches in subsequent chapters are based on the presented cost function.

3.1 Electricity Pricing

The price of electricity can be seen as a function of various variables, e.g. "costs of energy generation, transmission and distribution and consumer behavior" [8]. The dominant costs, the generation costs, are determined by the capital, operational and fuel costs [25]

$$C_{Total} = C_{Capital} + C_{Operation} + C_{Fuel} \tag{3.1}$$

The capital costs reflect the investment costs for a particular power plant. The operational costs represent the costs for maintenance and repairs to keep the power plant operational. Fuel costs reflect the costs for materials to power the electricity generation

Table 3.1: Cost Share of Different Energy Technologies [8, 26]

Technology	**Capital %**	**Operations %**	**Fuel %**
Coal	45	15	40
Nuclear	60	15	15
Natural Gas	35	35	30
Wind	65	35	0
Solar	75	25	0

[8]. Of course, this portion of the costs is free for renewable energy sources. Table 3.1 shows the cost split for different electricity production technologies.

The current cost structure for electricity only considers internal costs, also called production costs. These costs do not include costs for the environmental impact, e.g. health costs due to pollution from a coal plant. This is a major reason why renewable energy sources have difficulty proving their cost effectiveness. Chapter 4 will outline how external costs can be priced based on the environmental impact.

3.2 Electricity Trading

For completeness, and to understand the price development, this section will introduce the trading concepts behind electricity. According to Robinson and Khatib [27, 28], "electricity has important characteristics as an economic commodity". Compared to other commodities, electricity cannot be stored in large, market-affecting, amounts. Furthermore, because of the interconnections between the different customers and generation sites, the relationship between the two sites can be seen as a very complex system [27]. These days, the utility industry is undergoing a huge transition: from a regulated to a deregulated market [28]. The goal of this change is more efficiency in the electricity production and the introduction of competition to lower the generation costs [28]. According to Khatib [28], entities in this market can be “electricity producers, traders who do not own generation capacities, and electricity suppliers, which represents the customers in the market” (The supplier later sells the electricity to the customer). In a deregulated market, the relationship between demand and supply determines the price of the electricity. Figure 3.1 shows how the electricity price fluctuates over the course of one week.

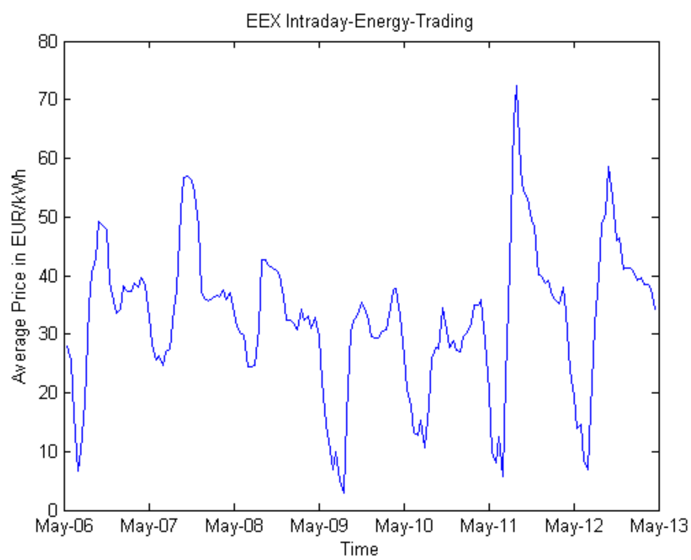

Figure 3.1: Average Trading Price at the European Electricity Exchange over One Week [29]

With the increasing penetration of renewable energy into the production mix, the generation shifts from a demand-driven production, in which the production follows the consumers demand for electricity, to a supply-driven production, in which the goal is to “harvest” all available renewable energy sources. Since the excess energy cannot be stored in a large scale, the effect of overproduction can cause imbalances. To avoid excess capacities, in some countries and states, operators of renewable energy plants have to pay balancing costs (as presented in Section 3.3).

3.2.1 Mid-Columbia Pricing

In this thesis, price data from the Mid-Columbia (Mid-C) Electricity Hub have been used to model the market behavior. The Mid-C hub is an "important electricity market hub in the northwestern United States", which is technically a 230kV transmission system [30]. Demand and supply at the hub form the Mid-C price, which is an important trading guideline for operations in the U.S. northwest. The data set was generously provided by Powerdex (Houston, TX), for research purposes, but because of the confidentiality of the data, actual values and plots cannot be shown.

3.3 Balancing Costs

It is controversial whether a high wind power penetration into the market leads to additional costs for integration. One side argues that a high wind power penetration needs more spinning reserves as a safety backup, and the ramping of wind power production causes extra costs for gas turbine operators. Ackermann et al. [31] found that increasing wind power penetration from 10% to 20% would raise the integration costs from 1 EUR/MWh to above 2 EUR/MWh for the Nordic electric grid.

In contrast, other publications by Boyle [3] and Dale et al. [32] argued that countries with high wind power penetrations, like Denmark or Germany, do not state additional costs for the integration.

However, for reasons of the grid stability, operators are interested in obtaining precise power production forecasts from the wind park owners. If the forecast is accurate enough, then conventional generation sources like gas turbines can be adjusted and extra costs can be avoided.

Therefore, the Bonneville Power Administration (BPA, Portland, OR) has a penalty scheme as incentive for the wind park operators in the northwest U.S. to create accurate forecasts. According to Alan Ingram's publication [33], any energy generation above the earlier-reported forecast is priced at 90% of the lowest price per MWh in the last 30 days, whereas a penalty of 10% of the highest price per MWh in the last 30 days is imposed on top of the current price if the production does not meet the forecast. This important penalty scheme is later used to establish a real cost function to evaluate the effectiveness of the designed controller.

3.4 The Cost of Wind Power

Usually there are three different ways to estimate the costs of wind power generation [26]:

- Cost per rated power of the turbine
- Cost per rotor size
- Cost of generated kWh

The first two measures are used to compare market rates of projects, whereas the last measure actually provides realistic cost information. Thus, this section will only concentrate on and show an example of the last cost measure. If the reader is interested in the other two indicators, Mathew [26] gives a good introduction to the cost of wind energy. According to Mathew [26], Cost/kWh is a good economic indicator. Hereby, the generated electricity and the cost of operation determine the cost ratio

$$
\begin{aligned}
C_{Generation} &= \frac{C_{Annual}}{E_{Generated}} \\
&= \frac{C_{Annual}}{8760 C_p P_R}
\end{aligned} \tag{3.2}
$$

whereby C_{Annual} are the annual total costs, $E_{Generated}$ the annual produced energy, C_p the average capacity factor and P_R the rated power output of the wind turbine.

It is visible that Equation 3.2 [26] considers the location-dependent capacity factor C_p. Hence, this measure gives a realistic ratio of cost-effectiveness.
Mathews [26] also points out that the net present value of the annual costs should be considered for the entire turbine lifetime, which is usually 20 years. Thus, Equation 3.2 should be extended by the net present value, $NPV(\dot{})$:

$$
\begin{aligned}
C_{Generation} &= \frac{NPV(C_{Annual})}{E_{Generated}} \\
&= \frac{C_{Investment}}{8760\ n}\left(\frac{1}{C_p P_R}\right)\left[1 + m\left[\frac{(1+I)^n - 1}{I(1+I^n)}\right]\right]
\end{aligned} \tag{3.3}
$$

whereby C_{Annual} are the annual costs, $E_{Generated}$ the produced energy in the entire year, $C_{Investment}$ the investment costs upfront, n the number of years of turbine lifetime, C_p the average capacity factor, P_R the rated power output, m the percentage of the initial costs, which determines the variable costs, and I the average interest rate for the expected lifetime.

Cost Example for a wind turbine In this paragraph, an example for the cost calculation will be presented. This example follows an older example by Mathew [26] with updated cost values from Wizelius [34].

In this example, the cost for a modern wind turbine is given as \$1.2M for a 1.0MW wind turbine [34]. According to Mathew [26], the starting cost for the installation and grid integration is given as 30% of the initial turbine costs. In addition to the "setup costs", further "costs for maintenance costs and land rent are assumed to be 3.5% of the turbine costs" [26]. The applied capacity factor is 0.35. The lifetime is expected to be 20 years. The interest rate for this lifetime is estimated as 6.5%.

The initial investment is calculated as the turbine costs plus the installation costs:

$$\$1.2M + 0.3 \cdot \$1.2M = \$1.56M$$

Applying equation 3.3 to this problem, the cost per kilowatt-hour can be determined.

$$\begin{aligned} C_{Energy} &= \frac{\$1.56M}{8760hr \times 20y} \left(\frac{1}{0.35 \times 1000kW} \right) \left[1 + 0.035 \left[\frac{(1+0.065)^{20} - 1}{0.065(1+0.065^{20})} \right] \right] \\ &= \$0.0353/kWh \end{aligned}$$

3.5 The Cost of Wind Power with Energy Storage

In comparison to the earlier-presented cost model, it is interesting how an investment in an energy storage system would influence the costs per kWh of the produced electricity. The additional system would increase the investment costs upfront. For simplicity, it is assumed that the storage systems need the same maintenance as the wind turbine, and the lifetime is also 20 years. In the present example, an energy storage system of a zinc-bromide battery is assumed.

For the battery storage, three factors determine the investment costs:

- Power rating
- Capacity rating
- Maximum number of battery cycles

John Yen [35] presented in his thesis that an energy storage unit for 1MW should be sized to a power rating of $0.2125PU$ and a capacity of $1.15PUhr$. The numbers are high, but they are also based on the simplest forecasting model with a forecasting horizon of one hour and no slope compensation.

A report of the Sandia National Laboratory on energy storage technologies [9] states the following prices for a zinc-bromide battery, which is favored by the energy systems research group:

- Energy Capital Costs = \$400/kWh
- Power Capital Costs = \$175/kW

Taking these sizing numbers and applying projected investment costs from the Sandia report [9], the initial investment costs would be increased to

$$\begin{aligned}
& \$1.2M + 0.3 \cdot \$1.2M \\
+ \quad & \$400/kWh \cdot 1.15PUhr \cdot 1MW \\
+ \quad & \$175/kW \cdot 0.2125PU \cdot 1MW \\
= \quad & \$2.057M
\end{aligned}$$

It is assumed that the annual maintenance costs of the battery storage are 3.5% of the associated investment costs and that all other factors are the same as in the previous example. Under this estimation, the costs per kilowatt-hour are:

$$\begin{aligned} C_{Energy} &= \frac{\$2.057M}{8760hr \times 20y}\left(\frac{1}{0.35 \times 1000kW}\right)\left[1 + 0.035\left[\frac{(1+0.065)^{20}-1}{0.065(1+0.065^{20})}\right]\right] \\ &= \$0.0482kWh \end{aligned}$$

The use of energy storage might be helpful to the grid power quality and safety, and might prevent fluctuations. However, the introduction of a zinc-bromide battery would increase the costs of electricity by roughly 36% (at a capacity factor of 35%, shown in Figure 3.2), which should be lowered to increase the acceptance of the storage idea. It is the main goal of this thesis to change how electricity is provided to the grid in order to increase the revenue to support the additional investments.

3.6 Determination of the Price Indicator

A critical step for the control schemes is the normalization of the control input values. For inputs to a neural network or a fuzzy controller (depending on the design), values are usually normalized to a range between -1 and 1. This criteria created an interesting problem in determining the best price indicator for the controller. If the "absolute price" per MWh is used as a sell/store indicator, the magnitude of the price determines the controller action. However, a high price during the winter could be relatively small compared to an electricity price during the summer, in which a supply shortage is usually observable. Due to the seasonal dependence of this indicator, the idea was discarded.

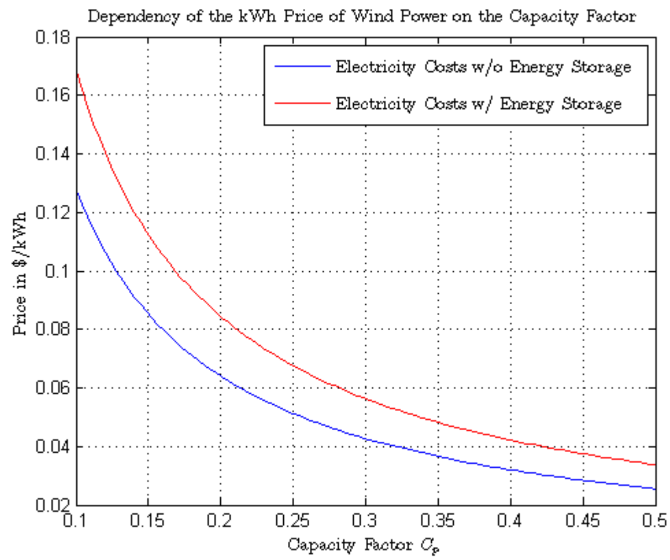

Figure 3.2: Price Dependency on the Capacity Factor for a Wind Turbine with and without Energy Storage System

Another idea was to take the price difference between time step t and t_{-1} as an indicator. However, it was observed that during different seasons the differences in the price can also vary. Finally, it was decided to use a relative price difference as an indicator. With relative price difference (RPD), the price difference is divided by the average of the price over the last week, as Equation 3.4 shows:

$$P_{RPD} = \frac{P_t - P_{t-1}}{\bar{P}_{last\ Week}} \tag{3.4}$$

3.7 Price Forecasting

A major component of the control strategy presented later is the electricity price development in the near future. The general idea is that it might be preferable to hold back saved energy in the storage system for a time when the price in the near future will be much higher and the revenue of the systems operation will also be higher. Thus, various forecasting methods have been investigated to determine the best performing method.

3.7.1 Persistence Model

In a persistence model, it is assumed that the forecasted relative price difference (F_{RPD}) will be the same as the current relative price change (P)

$$F(t+1)_{RPD} = P(t)_{RPD} \tag{3.5}$$

This naive method shows goods results for complex-behaving time series and "performs surprisingly well" [36]. It does not require any complex computation, and is therefore interesting for systems with limited computation possibilities.

3.7.2 Weighted Moving Average Model

Using a weighted moving average approach is a different method for price predictions, which was described by Song et al. [37]

$$F(t+1)_{RPD} = \frac{w_1 P(t)_{RPD} + \ldots + w_n P(t-n)_{RPD}}{\sum_1^n w_i} \tag{3.6}$$

As Equation 3.6 shows, the new forecast depends on n past price values, which are weighted by their influence on the next value (a value, which is closer to the current time step probably has a higher impact and is weighted higher than values, which are older).

3.7.3 Auto-Regressive Model

Another method presented by Song et al. [37] for price predictions, is the exponential smoothing method, which is an auto-regressive model.

$$F(t+1)_{RPD} = F(t)_{RPD} + \alpha(P(t)_{RPD} - F(t)_{RPD}) \tag{3.7}$$

Equation 3.6 shows that the next forecast depends on the current relative price change forecast and the weighted difference between the forecast and the actual relative price change. The constant α represents an adjustment factor that determines how strongly a forecasting error influences the next forecast.

3.7.4 Neural Network for Price Forecasting

Attempts were made to use a neural network for the relative price change forecasting. This method was recommended by Song et al. [37]. Neural networks have been quite successfully used in predictions of time series [38, 39].
However, the performance of the designed neural network in this thesis was not convincing and the mean square error was far off compared to the conventional models, due to a persistent offset between the price forecast and the actual value. Thus, it was decided not to pursue any further predictions with neural networks.

3.7.5 Comparison

The "controller to be designed" should have the capability of using price predictions for decision making. Therefore, it was of interest to investigate which of the presented methods actually performs the best and has the smallest mean square error and mean absolute percentage error. The goal was to compute both errors, because in the literature [38], both of these methods were used. It was of interest to see if the errors were actually different.

Therefore, the mean square error and the mean absolute percentage error (shown in Equation 3.8 and Equation 3.9) were calculated for all three forecasting methods, persistence, weighted moving average and, auto-regressive model, with a forecasting horizon from 30 min up to 6 hours (in 30 min increments). For the exponential smoothing method, two adjustment factors ($\alpha = 0.3$ and 0.7) were used to investigate the differences between a fast- and slow-approaching error correction.

Figures 3.3 and 3.4 shows the results of the comparison.

Mean square error:

$$E_{MSE} = \frac{1}{n}\sum_{t=1}^{n} |P(t)_{RPD} - F(t)_{RPD}|^2 \tag{3.8}$$

Mean absolute percentage error:

$$E_{MAPE} = \frac{1}{n}\sum_{t=1}^{n} \left|\frac{P(t)_{RPD} - F(t)_{RPD}}{P(t)_{RPD}}\right| \tag{3.9}$$

Both figures (3.3 and 3.4) show that, over most forecasting horizons, the persistence model provides a better performance than any other tested method. Thus, for the

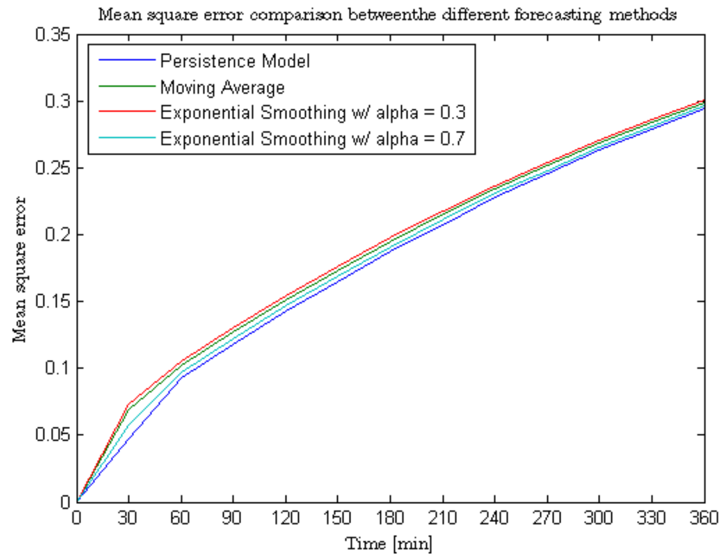

Figure 3.3: Comparison between the Mean Square Errors for Different Forecasting Horizons

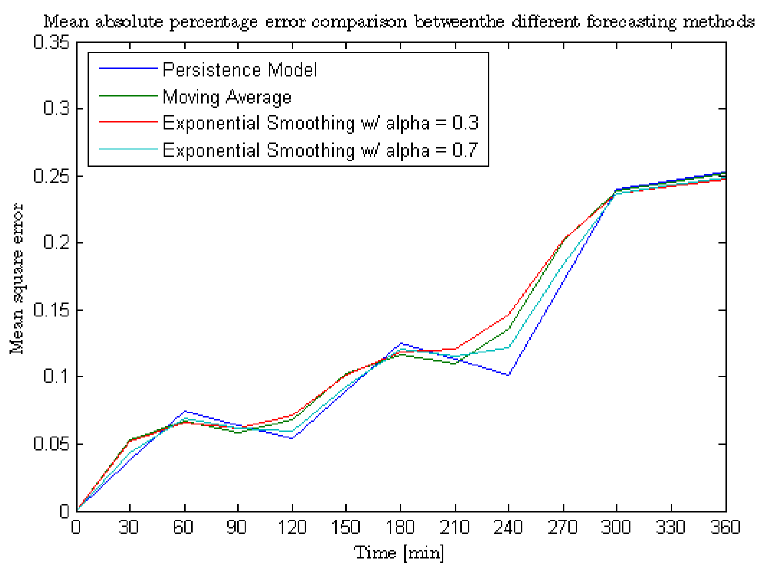

Figure 3.4: Comparison between the Mean Absolute Percentage Errors for Different Forecasting Horizons

following controller design, all price difference forecasts will be done by a persistence model.

3.8 Cost Function for the Optimization Process

The control strategy presented later will be optimized by a evolutionary algorithm. A key element of the algorithm is the evaluation of the performance of the control strategy by a cost function. This function determines the "fitness" or effectiveness of the found optimization solution. The idea was to design a cost function close to real world costs. Therefore, two principles were incorporated:

- The controller should have an incentive to sell electricity when the price is high. Therefore, part of the cost function is the overall produced electricity.
- All penalties for variations from the forecast (under or above) should be priced as in the real world. Therefore, the penalty scheme by BPA [33] (shown in section 3.3) is applied in the cost function.

Mathematically, the two principals can be presented as follows.
If the electricity generation is above the prediction:

$$J(t) = P_F(t) \times C(t) + (P(t)_G - P(t)_F) \times 0.9 \times C(t)_{under\ forecasting} \tag{3.10}$$

If the electricity generation is below the prediction:

$$J(t) = P(t)_G \times C(t) - (P(t)_F - P(t)_G) \times 1.1 \times C(t)_{over\ forecasting} \tag{3.11}$$

$J(t)$ is the total revenue at time step t, P_F and P_G the forecasted electricity production and the actual production respectively, $C(t)$ the Mid-Columbia Electricty price at time step t and $C_{underforecasting}$ and $C_{overforecasting}$ the penalty costs for under- or over prediction according to [33].

$J(t)$ is calculated for every time step and later totaled for the entire test period (April until December 2008). The revenue for the entire year determines the overall effectiveness of one particular controller solution.

3.9 Summary

This chapter introduced the basics of energy economy, explained how the price is established, and the electricity is traded. This chapter also addressed the costs of wind power production and showed how the price per kWh would roughly change if an energy storage system was included. In addition, the topic of balancing costs was briefly introduced.

Furthermore, this chapter explained why the relative price change is used as a price indicator, and why a persistence model is implemented for the price change prediction.

At the end of this chapter, the cost function for the later optimization process was introduced.

Chapter 4 – Life Cycle Assessment for Renewable Energy Technologies

With the ongoing discussion about global warming and the environment, the assessment of the environmental impact of services or goods becomes more important for decision making. Life cycle assessment (LCA) provides a methodology to analyze the "ecological foot-print" of a technological solution [8]. LCA is a "well-characterized methodology" [40], which is internationally accepted and defined through an international standard, ISO 14040 [41]. During the life cycle assessment, all product stages (material processes, manufacturing, life time and decomposition) are considered. Figure 4.1 shows all life stages for a modern wind turbine. In addition to the impact assessment, a life cycle analysis allows the impact comparison of two products, because the results of an assessment are product independent and are measured in eco-indicator points. A well-cited example for an LCA is the comparison between paper and Styrofoam coffee cups [42], where the environmental impact of both cups was investigated. The results of an LCA can be used to improve a service or product, because designs with a big environmental impact can be determined. This environmental improvement can have a great value for the business, because avoided waste is also avoided cost in the production stage, and goes hand-in-hand with the idea of lean manufacturing [43].

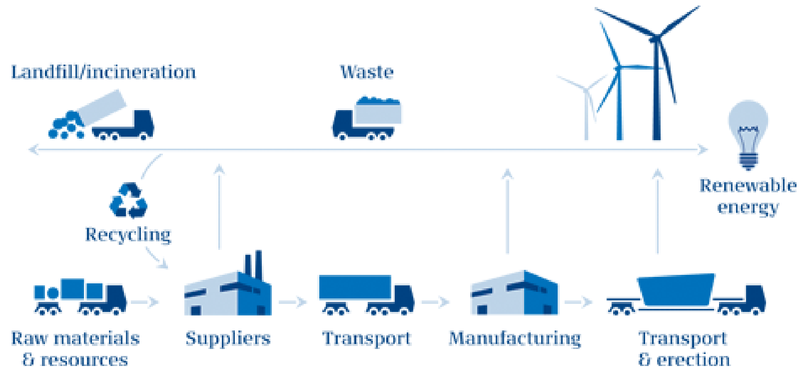

Figure 4.1: Life Stages of a Wind Turbine [44].

4.1 Using LCA to Determine Saved External Costs of Renewable Energy Technologies

The goal of this research was to investigate how an LCA can be used as a tool to determine the value of an investment in renewable energy. The main question was if the monetary value of emission savings can be assessed using life cycle assessment software. Of interest in the study was to investigate if infrastructure, aside from the wind turbines, have to be considered in a wind park LCA. An additional research task was the assessment of the impact of the wind turbine component reliability on the overall life cycle emissions. Before details of the assessment will be presented, the next section will give a brief introduction to the methodology of life cycle assessments.

4.2 Literature Review

Sources of renewable energy, like wind turbines or solar cells, belong to a small group of products that can have a zero or even a negative emission balance. Because of this fact, renewable sources have been previously investigated in regards to the life cycle impact. Schleisner et al. [45] presented an LCA study on wind turbines. Schleiser investigated the impact of a single wind turbine on the environment. However, the generator size of the investigated turbine was much smaller than today's modern wind turbines (the study investigated 500kW turbines). Schleiser presented one of the only studies, which considered the external costs to the public (for example savings through avoided pollution), which were saved by the project [45]. Jungbluth et al. [46] compared solar cells and wind turbines ($< 800kW$). Weinzettel et al. [47] investigated more modern turbines for an offshore project. The main focus was on marine ecotoxicity and regarding the energy production, generic capacity factors were assumed [47]. The most recent study on a modern wind turbine was published by Martinez et al. [48],but this study also only considers a single turbine. Assumptions were made about the capacity factor to calculate the energy payback time.

Another life cycle study was done by Pehnet [49]. LCAs are normally done in a static way, meaning that a fixed generation portfolio (coal, nuclear, gas, wind, solar, etc.) underlies the energy production. Pehnet investigated the effects on the life cycle impact, if the portfolio changes within the lifetime of the turbine (usually 20 years).

LCA is a viable and important tool for environmentally conscious companies. Turbine manufacturers regularly publish assessments for their turbines [50, 51]. It is hard to assess how many improvements are driven by LCA results, however, the results have been used for marketing purposes [52].

The main motivation for this study came from a study done by Lenzen et al [53]. Lenzen et al. investigated the location-dependence of assessments for renewable sources. The study compared locations in Brazil and Germany, and came to the conclusion that LCAs are highly location-dependent and results from a study in Europe likely will not accurately map to the U.S. Due to the location dependence of assessment, it was of interest to investigate a life cycle assessment for a wind park in Oregon.

All previous studies were either focused only on the wind turbine itself or on a very generic energy production of a wind park. Thereby, the studies were limited in their validity. The main motivation for this study was the access to real-world wind data. Thus, a realistic LCA could be performed for a wind park in northern Oregon.

4.3 LCA Methodology

In 1996, the first ISO standards for environmental assessments were published to guarantee comparability and objectivity. The ISO14040 and 14044 standards [41, 54] are guidelines for any accepted analysis. Every assessment consists of four major phases [41]:

- Definition of goal and scope
- Inventory analysis
- Impact assessment
- Interpretation

This is shown graphically in Figure 4.2.

Definition of Goal and Scope The definition of the goal and scope is important because it sets the expectation of what should be accomplished with the study (e.g., is the goal to compare two products or to determine the impact of one product). The first phase of the LCA also defines the functional unit, system boundaries, and the data quality standards. A functional unit is useful for a comparison of impacts between product parts; the system boundaries define what is specifically considered to be in

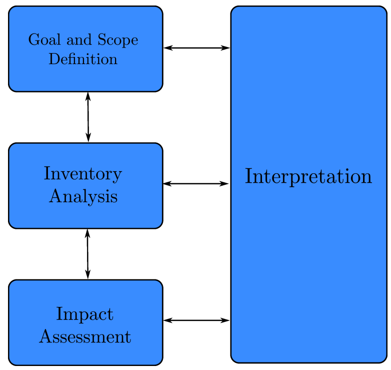

Figure 4.2: Phases of Life Cycle Analysis

the system; and data quality needs to be determined at the beginning because, for some studies, only data from specific databases can be used (e.g., European or U.S. databases) [55].

Inventory Analysis During the Inventory Analysis phase, data of sufficient detail about the material flow, the processes throughout the life cycle, and the disposal need to be collected. Once the data collection is finished, the system boundaries may need to be redefined. Since this step can be very complex, software tools like SimaPro (PRé Consultants, Amersfoort, The Netherlands) [56] or GaBi (PE International, Leinfelden-Echterdingen, Germany) **??** are used. The software helps with the access to databases, but also visualizes the impacts of product parts. In this particular study, the SimaPro [56] was was used.

Impact Assessment Once the previous step is completed, an impact assessment can be conducted. In this step, the impact is determined according to a life cycle impact assessment method. A method is chosen from the three most used methods [57]: the environmental design of industrial Products 1997 - EDIP97 [58], LCA - an Operational

Guide to the ISO standard - CML2001 [59] and Eco-Indicator 99 [60]. According to Dreyer [57], the first two methods are problem-oriented. That means they were very focused on one particular problem, in this case, it was toxicity, and do not consider "noise, land use, and fine particle matter" [54]. Eco-Indicator 99 includes several impact categories [54]. Since the results of the study should be comparable to other existing and future studies, Eco-Indicator 99, which is mainly used in LCA studies of renewable energy sources (e.g. [48]), was chosen. The Eco-Indicator 99 method allows assessing the collected data from three different perspectives listed below [60, 61].

- Egalitarian archetype
- Hierarchistic archetype
- Individualistic archetype

Since every data entry is afflicted with uncertainties, each perspective will weigh the uncertainty is a different way, e.g. Human Health has a more important impact in the individualistic perspective than in the Hierarchistic perspective. The perspectives are based on a survey done by an expert group from The Netherlands, Switzerland, and Germany [62]. According to Haapala et al. [61], the main differences lie in the time horizon of each assessment. The Egalitarian perspective for example aims for a long time horizon, whereas the Hierarchistic perspective combines "short and long time effects", and the Individualistic perspective only focuses on the short term impacts.

Concept of Impact Categories The Individualistic archetype considers *carcinogens (C), respiratory organics (RO), respiratory inorganics (RI), climate change (CC), radiation (R), ozone layer (OL), ecotoxicity (E), acidification/ eutrophication (AE), land use (LU),* and *minerals (M)* as impact categories [60, 61]. The Egalitarian and the Hierarchistic archetypes also consider *fossil fuels (FF)* in their damage assessment.

Table 4.1: Comparison Between Three Archetypes [60]

Perspective	**Time Perspective**	**Manageability**	**Required Level of Evidence**
I (Individualistic)	Short time	Technology can avoid many problems	Only proven effects
H (Hierarchistic)	Balance between short and long term	Proper policy can avoid many problems	Inclusion based on consensus
E (Egalitarian)	Very long time	Problems can lead to catastrophy	All possible effects

Concept of Eco-Indicator Points Results of the assessment may be calculated in SimaPro in terms of *Eco-indicator points*. According to the Eco-Indicator 99 Manual [60], an Eco-Indicator point (Pt) is defined as "one thousandth of the yearly environmental load of one average European inhabitant" [60].

Interpretation The forth and final phase of the life cycle assessment is the interpretation of the results. According to the ISO standards [41], "significant environmental issues should be identified" [60]. During this phase, recommendations and conclusions should be made.

4.4 Introduction to the Case Study

The goal was to investigate how a life cycle assessment can be used to assess the avoided environmental impact due to the operation of a wind park. Therefore, the idea was to use realistic data as much as possible, especially for the energy production. In the previous literature, generic capacity factors were always used in the LCA (e.g. in the life cycle assessment of Vestas [50], a capacity factor of 41% (onshore) was assumed). For a specific investigation on the emissions savings, this information was not precise enough. Fortunately, Portland General Electric (PGE, Portland, OR) granted the opportunity to used specific wind speed and power data to determine capacity factors. In addition, PGE supplied life cycle information on the wind park.

The following case is based on power data and information for a wind park in northwest Oregon with 100 Vestas (Randers, Denmark) turbines.

4.5 Problem Description, Goal, and Scope

The model for this LCA study is based a specific wind park in north Oregon with 100 Vestas turbines [1]. The Goal of the study was to investigate the specific avoided emissions due to the operation of the wind park and how the LCA can be used to determine the monetary value of the external cost savings. In addition, the impact of the turbine reliability was of interest.

For the scope of this study, the production of the individual wind turbines, the construction of the wind park (substation and transmission), the operational stage and the disposal stage were considered.

4.5.1 Functional Unit

As basis for comparison, the life time of 20 years was selected as functional unit. The unit can be seen as a baseline for the comparison between the wind park case with and without consideration of the turbine part reliability.

[1] Due to a non-disclosure agreement with PGE about the wind data, no specific information regarding the number of turbines or the generated electricity can be published. The actual number of turbines is different than used in this study.

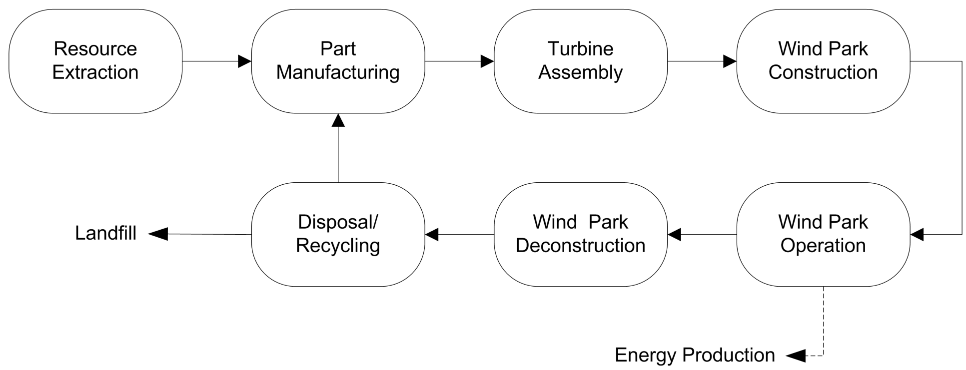

Figure 4.3: Life Cycle Inventory of the Wind Park

4.6 LCA Inventory

Figure 4.3 shows the LCA inventory for the entire turbine life cycle. The presented LCA includes all stages from the resource extraction (allocated in the ecoinvent database [63]), the part manufacturing, the turbine assembly, the wind park construction, the wind park operation and finally the recycling or disposal phase.

The material data was taken from the ecoinvent database [63] and was based on various material publications from the turbine manufacturer [50, 51]. The detailed list of used materials can be found in the Appendix.

4.6.1 Data Sources

The wind turbine component and part information, which are summarized in Table 4.2 and outlined in detail in Appendix, were gathered from various sources of the turbine manufacturer. The manufacturer released a company LCA report [?], which was used

Table 4.2: Weight and Energy for the Main Components of a Modern Wind Turbine

Component	**Weight**	**Amount of CO_2 in tons**
Blade (single)	7.40t	16.2
Foundation	832t	87.6
Gearbox	15.25t	51.6
Generator	9.09t	32.6
Hub/Spinner	20t	53.8
Int. Cables	0.8218t	2.5
Nacelle Shell	24.2t	36.4
Tower	135.2t	221.2
Transformer	3.091t	6.6

as a baseline for the main parts. Further information was gathered from the company environmental impact report [51]. Details on the blade manufacturing and material information were obtained from the environmental report of the Vestas factory in Isle of White, England, where blades are manufactured [64]. The following paragraphs will present details on the data which were used for this particular study.

Foundation The foundation is the heaviest part of a modern wind turbine. The 832t foundation should support the turbine, but also “act as a counterweight to prevent the turbine from tipping over” [34]. The size of the foundation depends on the soil condition, but a typical foundation is 2-3m deep and is square with side lengths of 7-12m [34]. Emissions from the concrete into the soil have not been considered in this study. The ecoinvent database profile for reinforced concrete was used for the concrete of the foundation.

Tower The tower is predominantly produced out of steel (126.1t), but other materials are used in small quantities and neglected in this study. With turbine heights of 80 and more meters, the tower is manufactured in sections of 20m length, transported to the wind park site and assembled on-site [34]. The paint for coating of the tower outside was neglected. The tower was modeled as ETH steel from the ecoinvent database.

Nacelle The nacelle of modern wind turbines contains the electric generator, gearbox, and the transformer. In the LCA analysis of the Vestas turbine, the mass and the used materials were only given for the entire nacelle [50]. This fact made it difficult to separate the materials for different nacelle components, especially to account for replacements due to reliability-caused failures. Weight information for the nacelle components were found in the environmental report for the Vestas turbine [51]. The relative masses of components have been used to allocate materials from the the Vestas life cycle report to each component [50].

Rotor Modern wind turbines use three blades [34]. Detailed information on materials used for the blades, hub, and spinner were obtain for the Vestas environmental statement [51] and sustainability statement of the blade factory at the Isle of White, England [64].

Wind Park Infrastructure The wind park examined in this study contained a substation with a main transformer. Furthermore, a grid connection to the nearest electricity grid of 50km was assumed. Construction of access roads was not considered, because local roads were already in place before the construction of the wind park.

Recycling and Disposal of Wind Turbine Components For this study, all recycling information were taken from the Vestas LCA 2006 report [50]. It states that 90%

of all steel, cast iron, stainless steel, aluminum and copper can be recycled. In addition, all plastic and glass fiber components are disposed at a landfill [50]. The foundation, including concrete and steel reinforcement, is assumed to be left in place.

4.6.2 Turbine Reliability

Reliability is an important issue for modern wind turbines. The length of the rotor blades has greatly increased due to recent developments. This technological enhancement gave the opportunity to produce more electricity, but it also caused more stress on major turbine parts like the gearboxes, generators, and blades [65, 66, 67]. Various companies have experienced turbine failures due to material fatigue before the end of the lifetime. A wind turbine is typically designed for a 20 year life [34].

In 1989, the German government established a “250MW Wind” program to investigate the failure rates of modern wind turbines across the manufacturers [68]. More than 1500 turbines were investigated; failures were reported to a “Scientific Measurement and Evaluation Program” database by the turbine operators. A study by Echavarria et al. [68] tried to determine the mean time between failure (MTBF) of main components per wind turbine based on this German data. The results from the study were used in this LCA to determine which and how many parts are replaced during the life time of 20 years (as reported in Table 4.3).

4.6.3 Assumptions and Limitations

The following assumptions and limitations were made:

- It was assumed that the turbine life time is 20 years.

Table 4.3: Number of Part Replacements per Turbine

Wind Turbine Component	**Est. Annual Failure Rate [68]**	**Est. Failure Rate over 20 years**
Nacelle	0.0025	0.05
Blades	0.024	0.48
Rotor	0.0045	0.09
Gearbox	0.012	0.24
Generator	0.022	0.44
Yaw system	0.005	0.1
Tower	0.0005	0.01
Transformer	0.002	0.04

- Due to the lack of detailed information on the transport of the turbine parts and construction of the wind park, the impact from the transport, final assembly impacts and construction was neglected. Martinez et al. [48] concluded that transportation-related impacts are "not comparable with the manufacturing phase, as it has a very limited effect".

- Manufacturing material and energy information within the ecoinvent database have been used to model turbine component production.

- Blades for a Vestas turbine contains balsa wood, it was not considered in this LCA. The amount of used balsa wood was unknown and an uncertain amount would have affected the study too much. Balsa wood has a major impact on the environmental balance and including an estimated amount would only distort the study. It was assumed that the amount of balsa wood used is minimal.

4.7 LCA Impact Assessment

Once all the material information of the wind turbine and the park auxiliaries are gathered in SimaPro, the impact assessment can be obtained. SimaPro provides various assessment options; only a few will be presented.

First, the environmental impact of a single wind turbine is presented, which is followed by a wind park assessment. Because of the balance between short- and long-term perspectives, the Hierarchistic archetype was selected for the Eco-Indicator 99 impact weighting [60].

4.7.1 Environmental Impact of a Wind Turbine

Figure 4.4 shows the total impact of the individual wind turbine components.

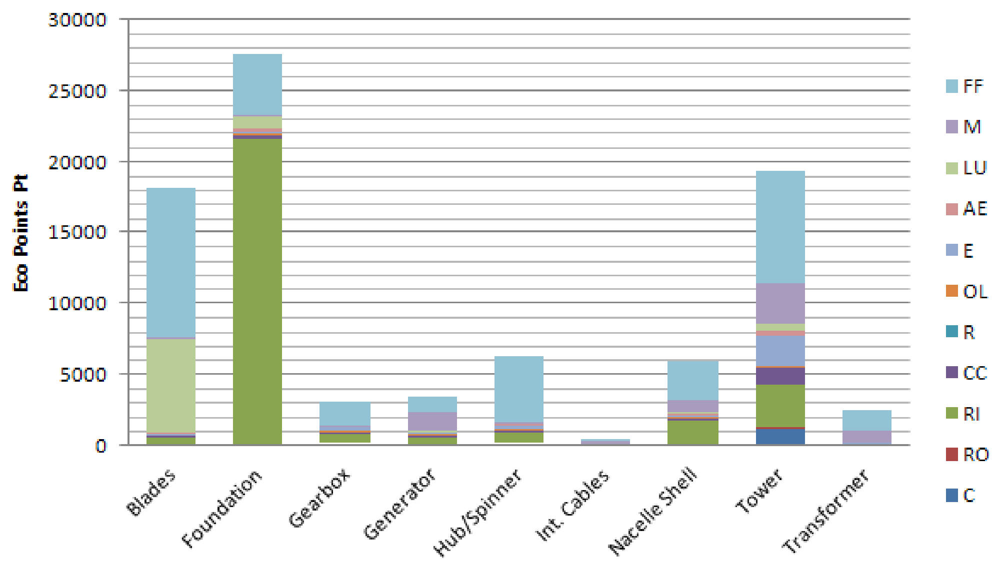

Figure 4.4: Life Cycle Assessment of a Single Wind Turbine. Information about the impact categories can be found in Section 4.3.

It becomes clearly visible that the wind turbine tower production, blade production and the foundation construction have the biggest environmental impact. The impact analysis of the foundation includes the land use for a single turbine and accounts for the lost surface area for natural sequestration. Furthermore, Figure 4.4 shows different environmental impacts of the components. For example, 1/3 of the blades' environmental impact comes from the impact on land use. Because in this particular blade type, actual wood is used (balsa and birch wood), the land use accounts for the deforestation. The stated results for a single wind turbine are similar to previous published LCA results [48].

4.7.2 Environmental Impact of a Wind Park

Figure 4.5 shows the inventory network for an entire wind park. The graphics shows the assembly stages (blue), the wind park life stage, and the recycle/disposal impact. The red line between the stages mean that the last process had a negative environmental impact. Green connections symbolizes a positive impact, or an avoided impact, of the process. This can be observed with the recycling process, because the majority of the turbine parts are recycled and therefore virgin material can be avoided in the production.

Figure 4.6 shows the environmental impact of a wind park, which is in operation for a life time of 20 years. Figure 4.6 demonstrates well that wind turbines belong to a small group of products that can actually offset their emissions from the production and disposal phase and create a negative balance (a negative balance always means avoided environmental impacts). An impact of 7.7MPt from the turbine production (shown in Figure 4.7) faces an offset of over 230MPt during the wind park operation. Interestingly, if the reliability of the wind turbine components is considered, it leads to an increase

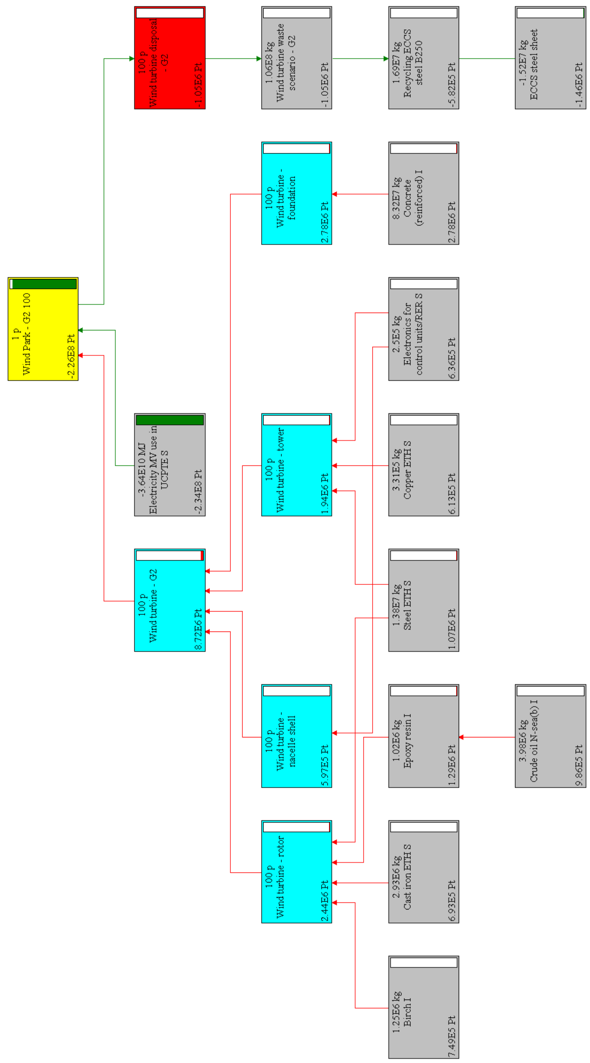

Figure 4.5: Life Cycle Inventory Network of a Wind Park

of the production impact of 6.8% and it reduces the avoided environmental impact of the entire life time by 0.24%. This calculation shows that the additional impact of the reliability on the turbine component production is very small in comparison to the avoided emissions during the 20 year lifetime, and therefore can be neglected.

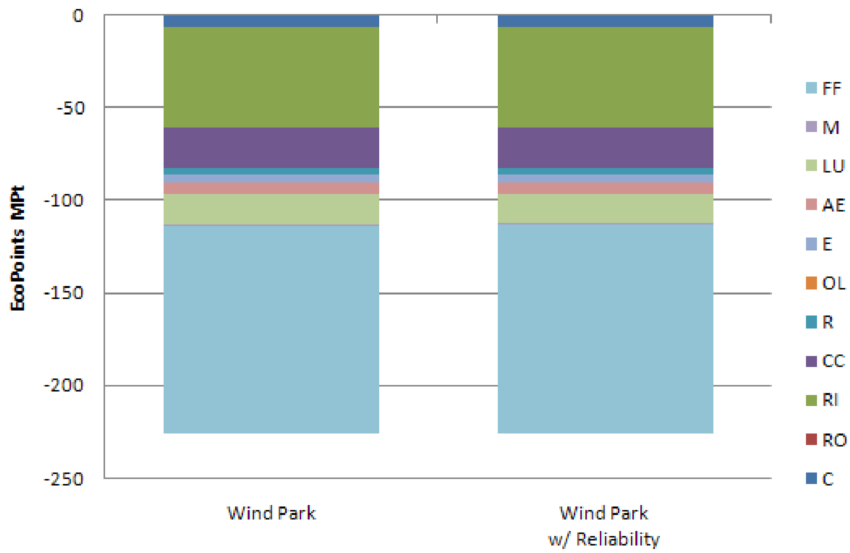

Figure 4.6: Life Cycle Impact Assessment of a Wind Park over a Life Time of 20 Years

4.7.3 Influence of the Capacity Factor on the Environmental Impact

The influence of the turbine's capacity factor on the environmental impact of the farm was also investigated. Figure 4.8 shows the impact results for capacity factors of 25%, 30%, 35% and 40%. The capacity factor is the ratio between the actual produced power compared to the designed power rating (nameplate) over a year. The capacity factor C_p can be calculated as follows:

$$C_p = \frac{E_{Produced}}{8760 \times P_{Rated}} \tag{4.1}$$

As shown in Figure 4.8, smaller capacity factors lead to a smaller positive environmental impact. It should be noted that the relationship between the capacity factor and the environmental impact is linear.

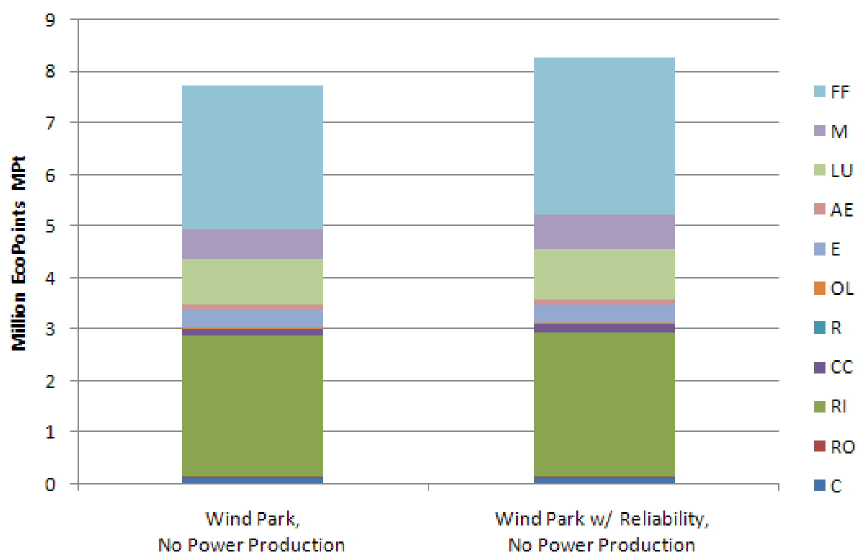

Figure 4.7: Life Cycle Impact Assessment of a Wind Park neglecting Energy Production over a Life Time of 20 Years

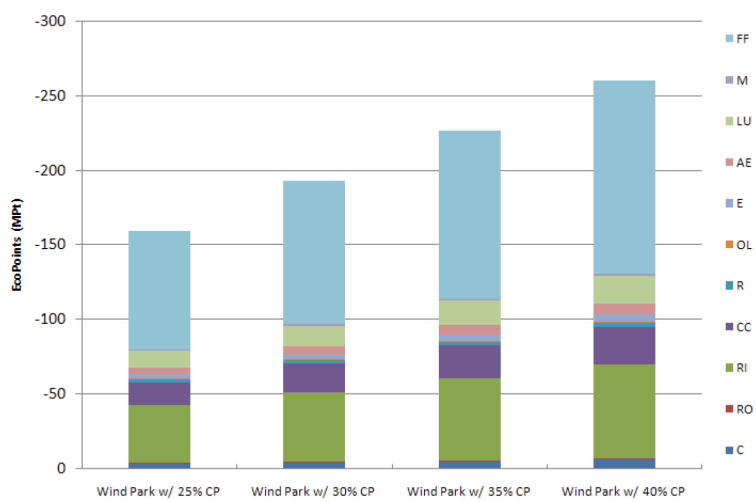

Figure 4.8: Life Cycle Assessment of a Wind Park with different Capacity Factors

4.8 LCA Recommendations

Based on the presented life cycle impact analysis, the following recommendations for improvements around the wind turbine and the wind park can be made:

- The usage of natural resources like balsa wood leads a high impact due to deforestation. If possible, these materials should be avoided, even though the production might be more expensive.
- After construction for the wind turbines, the footprint of each turbine should be covered with vegetation to allow more natural sequestration.
- The emissions from the foundation's concrete to the air should be reduced through a kind of containment system to avoid respiratory inorganics.
- The main substation of a wind park should be placed central to all wind turbines to reduces copper in the cables, but the substation should also be not too far away from a road to limit the extra construction and to limit the sealed surface area.

4.8.1 Energy Payback Time

The energy payback time is an important measure for renewable energy sources. The payback time states after how many months or years the same amount of electricity is generated as was used during the production. Table 4.4 shows the amount of energy needed to produced one wind turbine or a wind park with 100 turbines.

The results of Table 4.4 lead to a payback time for a single wind turbine of 8.8 months. This means that after 8.8 months, the wind turbine produced the same amount of energy, which was needed for its production. The time increases by 7.9% to 9.5 months if the

Table 4.4: Used Energy for the Production of a Wind Turbine and Wind Park respectively

Life Cycle Case	**Energy in MJ**	**Energy in MWh**	**Payback Time in Month**
Wind turbine	1.34×10^7	3728	8.8
Wind turbine with reliability consideration	1.45×10^7	4025	9.5
Wind park	1.06×10^9	294522	6.9
Wind park with reliability consideration	1.14×10^9	317372	7.5

reliability of the wind turbine is considered. If an entire wind park with 100 turbines is considered, then the payback time is 6.9 months and 7.52 months, respectively if the failure rate is not or is considered. All calculations were done under the consideration of a lifetime of 20 years and a capacity factor of 36%.

4.9 Using LCA as a Business Tool

The development of renewable energy projects is extremely capital intensive. Therefore, investors are looking for further revenue streams once the project is in operation.
A new emerging revenue stream is the sale of emission allowances due to the fact that renewable energy sources do not emit greenhouse gases. These allowances can be traded like normal stocks and, in the future, will depend on the market price of carbon.
This section explains the existing and future trading markets for carbon emissions and later it will be shown how a life cycle assessment can be used to assess the value of the emissions saving.

4.9.1 Current Carbon Market

"A central feature of the Kyoto Protocol" [69] is the emission reduction from electricity generation. The treaty initiates three major "market-based mechanisms" to enhance the reduction:

- Joint Implementation
- Clean Development Mechanism
- Emissions Trading

In the following sections, a summary of the existing trading mechanisms for greenhouse gases is presented. Later, proposals of future emissions trading are introduced to give an example for the importance of a life cycle assessment for renewable energy technologies.

4.9.1.1 Joint Implementation

Most of the mechanisms that are already in place for emission trading are aimed to help countries to achieve the Kyoto emission reduction obligations. As a example, joint implementation is a tool for industrialized countries to achieve their targets "through investments and the development of projects in other countries" [70]. In return, the initiating country receives Emission Reduction Units (ERUs), which count toward the Kyoto goal of the country [70].

4.9.1.2 Clean Development Mechanism

Clean Development Mechanisms are another tool of the Kyoto protocol, where project developers are allowed to receive "certified emission reduction (CER) credits" [69] if they invest in countries where the emission reduction can be achieved more cheaply than in their own country. The received credits "can be traded and sold" [69] and also count toward the country's obligation to reduce the emissions.

4.9.1.3 EU Emission Trading System

The EU Emission Trading System is "the largest multi-country, multi-sector Greenhouse Gas Emission Trading System world-wide" [71]. Currently 27 European countries participate in the system, which sets emission limits for different industry sectors and allows excess to be traded among different companies.

4.9.2 Future Carbon Markets

All of the existing measures try to incorporate the external costs of the greenhouse gas emissions. But in many cases, the real external costs are not priced into the product or service. To enhance a more eco-conscious behavior, ideas are currently proposed to account for all production costs (internal and external costs):

- Cap and Trade
- Carbon Tax

4.9.2.1 Cap and Trade

In a "cap-and-trade" system, "mandatory caps on emissions" [72] are established by an overseeing agency (e.g. in the U.S. it would be the Environmental Protection Agency) and companies that have excess carbon permissions could trade them with other companies that have exceeded their allowances. This trade is an incentive for companies to reduce emissions and provides them with a possibility to gain capital gain from selling these allowances to other companies.

Currently (May 15th, 2009) a bill is being discussed in the House of Representatives that would establish a cap-and-trade system for U.S. [73]. Independent from the federal bill, states like Oregon are also moving forward to establish a state cap-and-trade system [74].

4.9.2.2 Carbon Tax

Another way to account for greenhouse gas emission is a carbon tax, which would create a tax representing the amount of carbon (or equivalent other greenhouse gases), which was produced during the manufacturing of a product. The idea is that companies would try to reduce this tax through the reduction of greenhouse gas emissions [75]. This system would include all products and services, and would avoid complexity and exclusions for some products [76]. However, to date, in no country has made the legislative attempt to introduce such a tax.

4.9.3 LCA as a Business Tool

The previous sections explained that emission saving can be traded like other commodities on the daily market. But to make this trading possible, the emission saving of the renewable energy technologies have to be assessed.

A life cycle assessment, according ISO14040 [41], provides a standard assessment, which not only determines the carbon emissions, but also any major greenhouse gas emission, and provides generality and comparability if the assessment is based on the same life cycle inventory database, like the Swiss ecoinvent database [63].

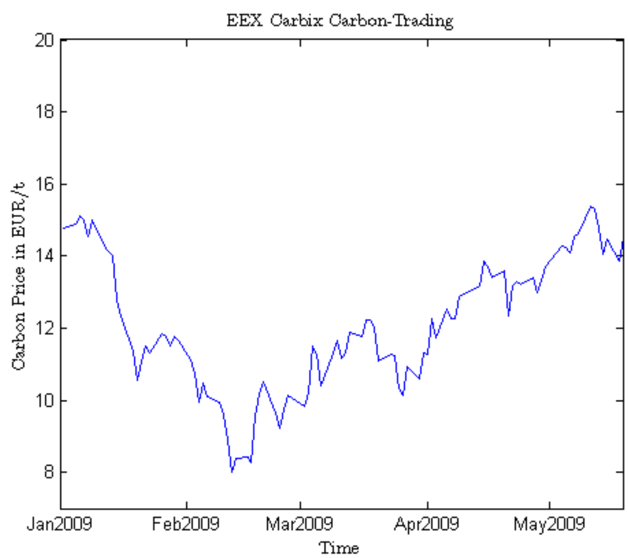

Figure 4.9: Trading Price of Carbon Emissions for 2009 at the European Energy Exchange. Data taken from [77]

Figure 4.9 shows the development of the price for carbon emissions at the European Energy Exchange in Leipzig, Germany over the period from January to the end of may 2009. Avoided emissions could be traded at any time at the current market price. In order to determine the value of the emission saving through the use of renewable energy sources, the study suggests the following five steps on an example for a wind park:

Step 1 Determine general information about the renewable energy project, which includes collecting material information from the turbine manufacturer.

Step 2 Gather project specific information. This should included how the wind park area was used before the park construction. Try to determine the area of land that was changed because of the construction.

Step 3 Model the wind park construction based on Step 2 with a recognized LCA software.

Step 4 Examine a full life cycle assessment of the wind park, including the environmental impact assessment.

Step 5 Confirm your results through an independent reviewer. The review should include a confirmation that the study was performed according to ISO14040 and ISO14044 and that only standard inventory databases were used.

Once these steps are performed and confirmed, the exact value of the saved emissions can be put on the market for a bid or sold at the current market price. If this practice would become standard, sold emission savings would be comparable and objective.

In May 2009, the U.S. Environmental Protection Agency introduced mandatory life cycle assessments for bio-fuels if companies apply for grants or subsidies [78]. This is just one example that life cycle assessments will become a business tool and standard.

4.10 Summary

The chapter introduced the methodology of life cycle assessment for renewable energy technologies. Furthermore, a life cycle assessment of a wind park in northwest Oregon, U.S. was presented and the impact of the turbine reliability investigated. It was concluded that the impact of additional parts for one wind turbine can be neglected for the life cycle assessment, because of extremely small impact if the energy production of the entire life cycle is considered. Later, the current and future carbon trading possibilities were introduced and it was explained how a life cycle assessment can be helpful to determine the value of the saved emissions.

Chapter 5 – Implementation

This chapter explains how the neural network, the fuzzy logic controller and the genetic algorithm were implemented and modified for this control problem. Furthermore, the chapter shows how the algorithms were tested for proper function.

5.1 General Idea

The general idea was the development of a controller that decides whether energy is stored in an energy storage system or energy from the system is used to offset a lack of wind power. Figure 5.1 shows that the controller is placed between the wind park

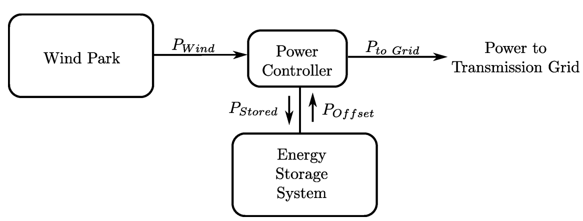

Figure 5.1: Power Flow between the Wind Park, the Energy Storage System and the Power Grid

power output, the energy storage system and the grid connection. Since it is technically impossible to store enough energy to balance out large fluctuations so that the wind park power output looks like a constant base load, the goal is to use the energy storage to balance out differences the between the wind power production and the forecast of the power production for the same time step. Operators of wind parks are committed to provide the grid authority. In the case of this thesis, it is the Bonneville Power Administration, with a one-hour wind power forecast. These forecasts can be based on similar methods as those presented in Chapter 3. However, currently only a one-hour persistence model is used to predict the produced wind power [79]. Figure 5.2 shows an example of a wind park output and its forecast over the course of 5000 minutes (roughly 3.5 days). It also shows that the persistence model is always lagging a little behind the

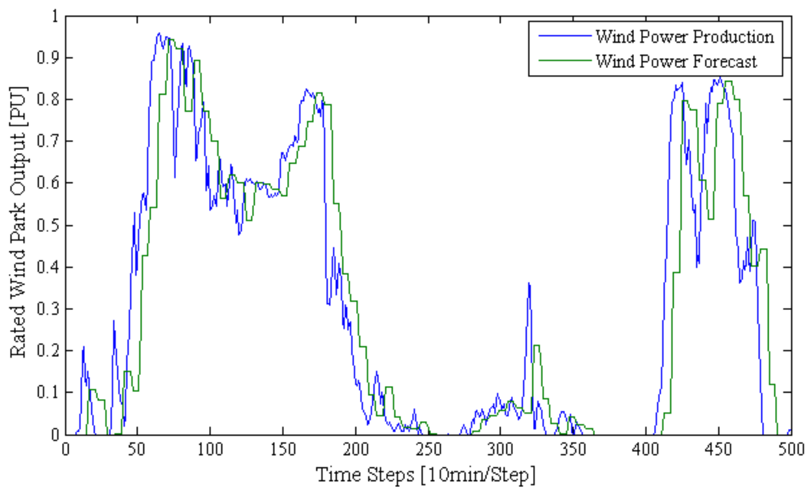

Figure 5.2: Rated Wind Park Power Output and its Forecast

actual power production, since it assumes that the current power level will be the same in an hour. Also visible in Figure 5.2 is the ramping between different forecasts. BPA's forecasting model averages the last hour's wind park power and projects it for the next hour. However, to avoid step changes, the forecast "ramps" from one forecast level to the next forecast, starting ten minutes before the start of the next operating hour until ten minutes after the start of the operating hour.

The power difference is based on the power production and the power forecast for each time step, and can be simply stated as

$$P_{Difference}(t) = P_{Production}(t) - P_{Forecast}(t) \tag{5.1}$$

Since the goal is to minimize the power difference with the use of the energy storage, the difference will be one of the input variables for the controller. The range of this indicator is normalized to the maximum wind park capacity and can range from -1 to 1.

Another important controller variable is the state-of-charge of the battery. It represents the level of available capacity normalized to the maximum capacity of the battery. It indicates how much capacity is available at the time step t. This variable is already normalized by the maximum battery capacity to a range between zero and one. However, for use as an input parameter for the neural network or fuzzy logic controller, the values were shifted to a range between -1 and 1.

A key element of the to-be-designed controller is the consideration of the electricity price. It is envisioned that the controller could deny offsetting a power difference if the price is low at time step t and it is anticipated that the price will rise in the near future. The profit from the shifted sale of electricity could be used to recover the extended costs for the energy storage system. Figure 5.3 shows the idea visually.

Therefore, two further controller input variables were considered: the relative price change of the electricity market price at time step t and the predicted relative price change in the future (see Section 3.6 for details on why the relative price change was chosen as a price indicator). Since a persistence model was chosen for the price prediction, the time horizon does not have to be specifically defined. However, it is assumed that

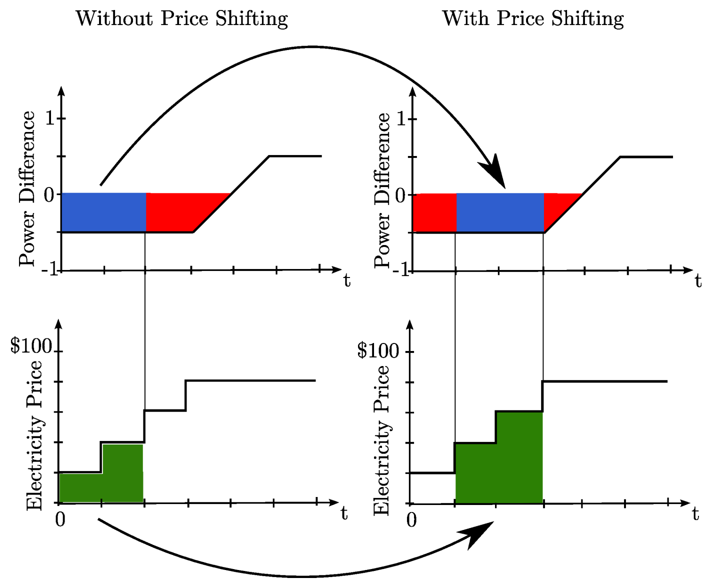

Figure 5.3: Benefits of a Shift in Energy Sale from the Energy Storage System with a power rating of 1PU and capacity rating of 1PU hr

the forecast is done for a time frame of one or two hours. In order to standardize the price variables, all price time series have been normalized to values between -1 and 1.

In summary, the controller inputs are:

- Battery state-of-charge (SOC)
- Wind park power difference
- Rel. price change at time step t
- Rel. price change at time step $t + x$

It was envisioned that the controller would decide if excess energy should be stored, a deficit should be offset, or the energy storage system should not interact between the wind park and the grid at time step t.

This idea leads to three discrete states from which the controller can choose its output:

Store Excess energy should be stored

Sell Offset energy should be provided to the grid

Hold The energy storage system does not interact between the wind park and the transmission grid

All controller inputs and outputs are summarized in Figure 5.4.

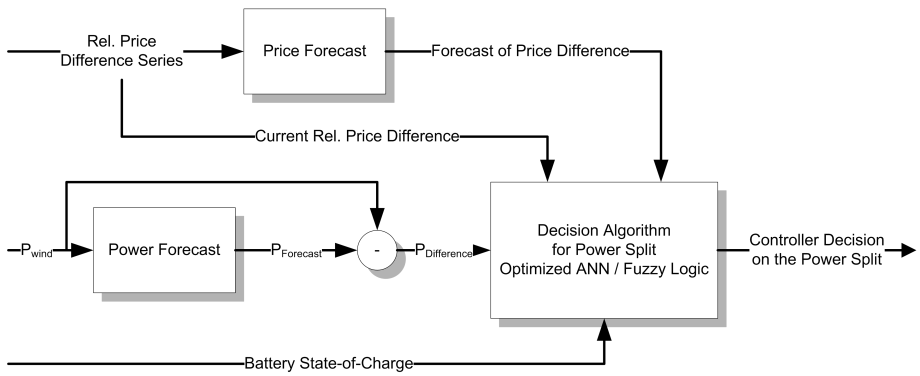

Figure 5.4: General Controller Overview

To obtain the optimal decision about the power split, it was envisioned that the controller would determine the optimum by itself and only rely on a minimum of expert knowledge. Therefore, the concepts of neural networks and fuzzy logic were chosen because both methods allow optimization with genetic algorithms [11]. The implementation of the concepts will be explained in the following sections.

5.2 Implementation of the Neural Network Control

The neural network was implemented in a MatLab (Mathworks, Natick, MA) script as a matrix implementation according to Rojas [17]. Functions of the MatLab neural network toolbox were not used.

The realized network is a multi-layer feed-forward network with a structure of four input neurons (one neuron for each input variable), two hidden neurons and one output neuron. Figure 5.5 shows the structure of the network.

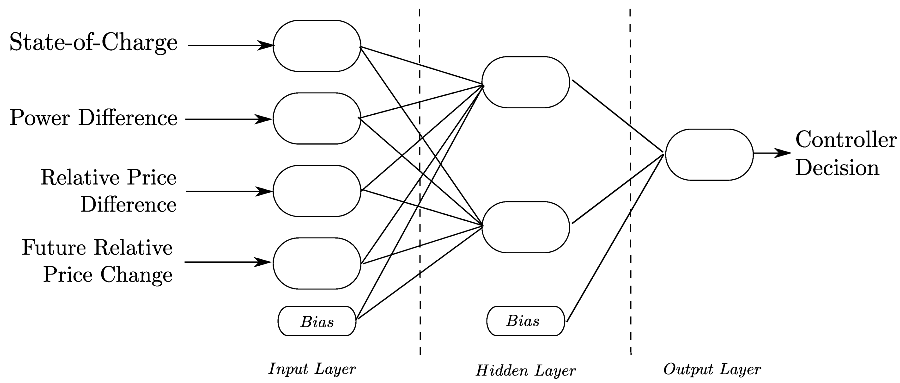

Figure 5.5: Implemented Multi-Layer Neural Network Structure

It was decided to use the "backpropagation" algorithm with gradient descent as presented in Chapter 2 for training the neural network. The training of the network showed the best results with a hyperbolic tangent activation function for all hidden neurons and a linear activation function for the output neurons (the training results performed better than a network with a sigmoid function).

Because the neural network is supposed to find the optimum of the power split without much human interference, it was decided to split the training into two phases. During the first phase, the network was trained supervised based on 16 extreme cases (The training set can be found in the Appendix). The cases originated from all combinations of extreme inputs (like SOC high, Power Difference high negative, Rel. Price Change high, Future low, etc. leading to 2^4 combinations). The network was trained with a maximum of 1000 epochs on this dataset. A training that converged to an error below a maximum error rate for the last 20 epochs was finally selected for the next step. If a training exceeded the maximum number of epochs, then the weights were discarded and the training was restarted. The second step, the "fine tuning", was designed to be unsupervised. Weight adjustments were performed by an genetic algorithm, which is presented in the following section.

It is important to mention that, in the actual controller, the output signal is discretized after it is computed by the network. A threshold *Price limit* is given to the controller, above which the controller output is discretized to "Sell", below the negative threshold it is translated to "Store", and in between the result is interpreted as "Hold". These "Action Labels" cause the action of the controller.

5.2.1 Test of the Neural Network Implementation

It is difficult to debug a neural network implementation because of the randomness of the network weights. To deal with this problem, the implementation was tested on an Exclusive-OR problem. The test was performed with the same neural network algorithm. The number of input neurons was adjusted to only two inputs. The XOR problem is a common test for a three-layer neural network [24]. If the inputs are plotted on a surface, the area could not be split into two regions for $Y = 0$ and $Y = 1$. Therefore, the problem can only be solved by networks with three or more layers [80].

Figure 5.6 shows the successful reduction of the learning error over a period of 10000 epochs. After the training was completed, the network calculated the exclusive OR output for the given inputs (shown in Table 5.1), and the results for this test can be seen in Figure 5.7.

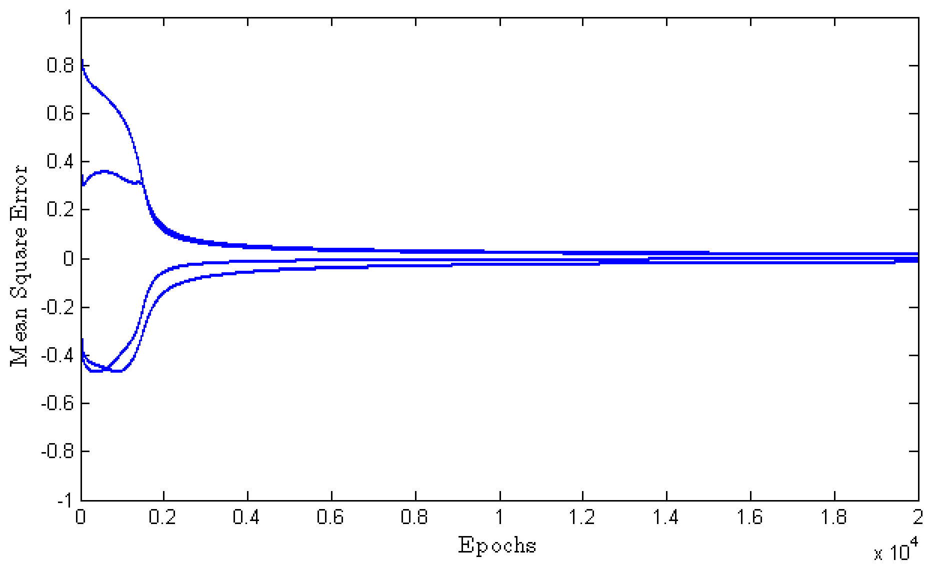

Figure 5.6: Development of the Learning Errors for Each Presented Input Pattern over a Time of 10000 Epochs

5.2.2 Optimization of the Neural Network

The second training step was done by a genetic algorithm. A set of training weights was reshaped into a vector that represented the solution chromosome. For a network with the presented structure (4,2,1), the hidden weights are represented by a 4×3 matrix, and the output weights are represented by a 3×1 matrix (all weights including the biases).

Table 5.1: Boolean Table for XOR Combination

X_1	X_2	**Y**
0	0	0
0	1	1
1	0	1
1	1	0

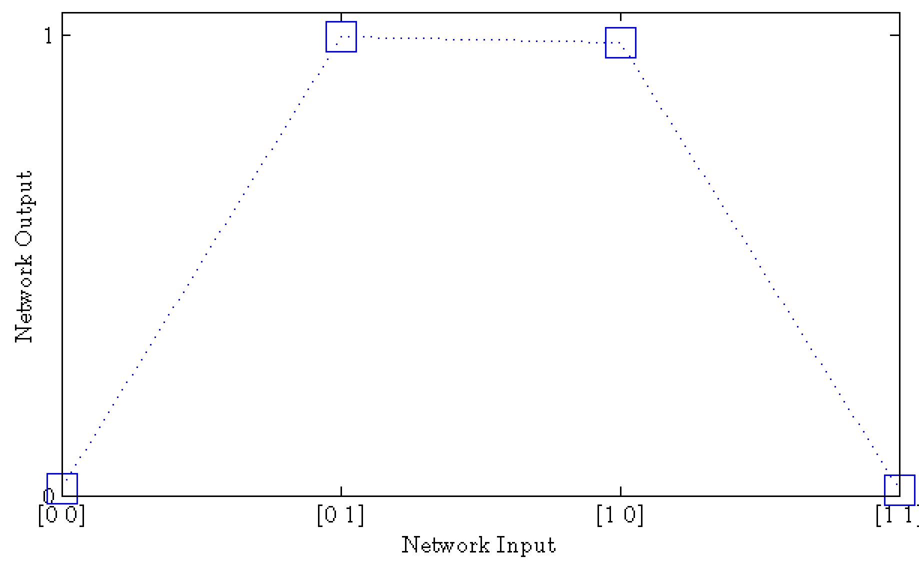

Figure 5.7: Results of the XOR Neural Network Test

Thus, a chromosome with a length of 15 values is created. Figure 5.8 shows an example of how the weights are reshaped into a chromosome.

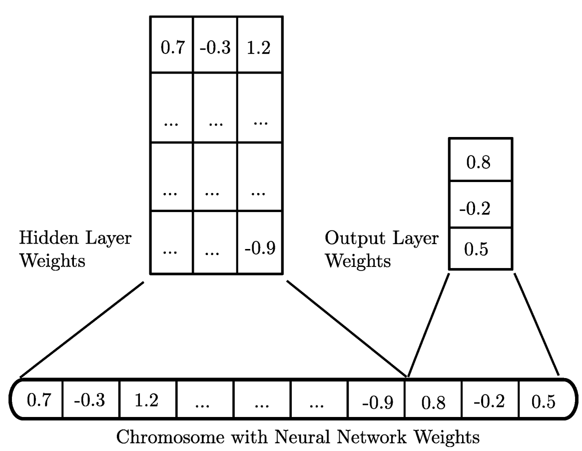

Figure 5.8: Example for Distribution of Network Weights in a Chromosome

As part of the genetic algorithm, three manipulation functions were developed based on the explanations in Chapter 2.

Cross-Over Two random chromosome parents create a new chromosome based on a random cut of their own chromosome.

Mutation A new solution is created through a mutation of a parent chromosome part by a random value. The mutation function determines the number of mutated chromosome parts, mutation range (by which random value the old value is altered) and the probability distribution of the mutation range (Gaussian or normal distribution)

Selection Based on the fitness of each chromosome, a fixed number of the best solutions is selected to become the next generation of parent chromosomes.

5.2.3 Test of the Implemented Genetic Algorithm

Zak [21] presented a test for genetic algorithms, which was used to test the implementation. As shown in Figure 5.9, the function

$$J(x) = -15(\sin(2x)^2) - (x-2)^2 + 160$$

has a lot of local maxima in the range from -10 to 10. The goal of the genetic algorithm was now to find the global maximum. Therefore, the range from -10 to 10 was split into 1000 discrete bins, each represented by a 10-bit number. To start, ten parent solutions were randomly generated and then genetically manipulated over a course of 1000 epochs. The results of this test can be seen in Figure 5.10 and show that a random solution of the first chromosome generation was already very close to the optimum, and over a course of 150 epochs, the maximum of 159.8 was reached. If the set of values would have been swept linearly, it would have taken almost 600 epochs (it is important to note that a maximum earlier in the range from -10 to 10 would have led to a smaller number).

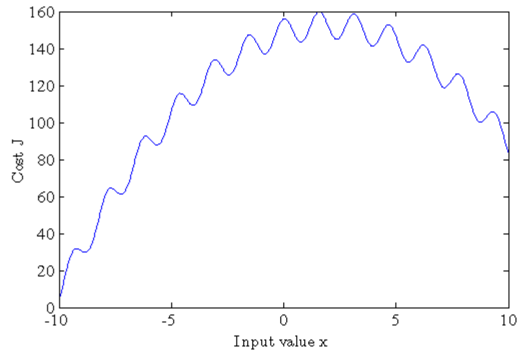

Figure 5.9: Test Cost Function

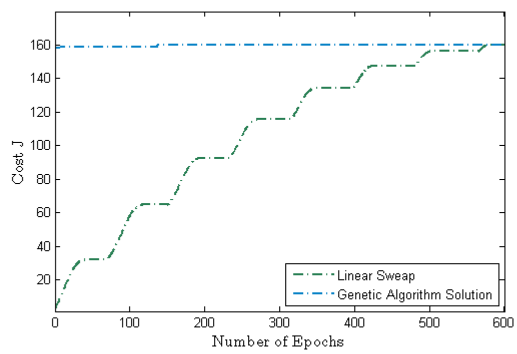

Figure 5.10: Optimization Results over a Course of 600 Epochs

5.2.4 Optimization Procedure for the Neural Network

To develop an optimal solution for the neural network controller, ten weight sets were created through supervised training with the extreme cases. If a training terminated before a maximum of 1000 epochs and the total training error was below a given threshold, then the weight set became a parent solution. If a training did not meet this criteria, then the solution was discarded and the next training started.

Once the training of ten solutions was finished, the actual optimization with the genetic algorithm started. As explained, hereby previous solutions are manipulated in order to achieve a better solution. It has to be noted that the manipulations of the network weights were not constrained to a limit because network weights could theoretically reach any value. Once a new pool of chromosomes was generated through mutation, cross-over and selection, all solutions were evaluated to determine their fitness. To do so, their performance as a controller was tested on a small data set of 2500 data points. The ten best chromosomes (the ten solutions that lead to the highest revenue) of this generation were then saved and became the next generations parents, which were manipulated. Figure 5.11 shows the flow chart of all actions.

5.3 Implementation of the Fuzzy Logic Control

The fuzzy logic controller presented in Chapter 2 was also implemented as a MatLab script and without the usage of any toolbox. To reduce the number of fuzzy rules to cover the entire solution space, it was decided to limit the number of membership functions to three: low, medium, and high (in the case of the power difference, it is negative difference, no difference, and positive difference). Because of the Zak's recommendation [21] to center the membership functions around zero in order to simplify the later optimization, the membership functions were spread out between -1 and 1. The advantage is that the neural network uses the same input ranges due to the hyperbolic tangent activation function.

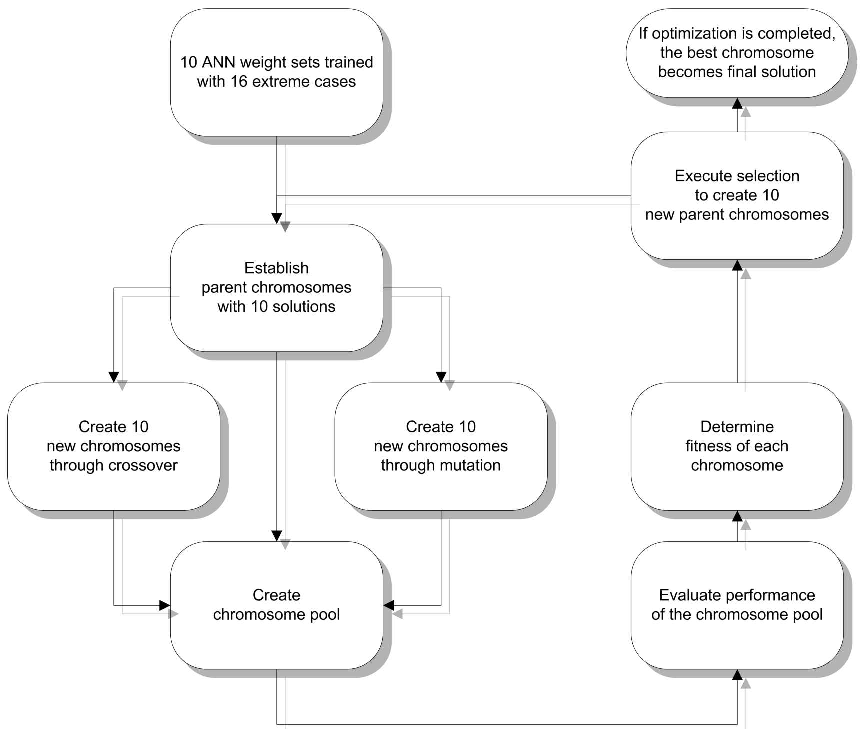

Figure 5.11: Flow Chart of the Optimization Procedure for the Neural Network Controller

A fuzzy logic controller with four inputs and three membership functions each needs 81 fuzzy rules to cover all possible input combinations ($3^4 = 81$). These rules, which are AND conjunctions of the input parameters, were predetermined by the author and can be found in the appendix to this thesis. Depending on the fuzzy rules, each input set is evaluated and the output is determined. Because a fuzzy logic controller can be debugged easier than a neural network controller, it was not chosen to test the implementation. Identical to the neural network controller, the output of the fuzzy controller was also discretized into the “action labels” “Sell”, “Store” and “Hold”.

5.3.1 Optimization of the Fuzzy Logic Controller

Due to the symmetry and the limits of the membership functions, all membership functions of one variable were determined by only one value. The "low" membership function peaked at the negative amount of this value and was bounded by -1; the "medium" membership function always peaked at zero and started and ended at the negative and positive value due to the symmetry; and the "high" membership function peaked at the positive amount of the value. Therefore, a chromosome for the fuzzy logic controller optimization was only four values long. For the optimization process, one initial set of membership functions was determined by an expert and nine further sets were randomly created. As shown in Figure 5.12, the optimization process of the fuzzy logic controller was similar to the optimization of the neural network controller with the difference that chromosome values were limited to a range between -1 and 1 due to the limits of the membership functions.

5.4 Test System

Because the real simulation deals with various random time series, the neural network and fuzzy logic controller were tested on an artificial system. Prices and power differences were modeled as sine functions, which had the advantage that values did not need to be normalized and that the behaviors of price and power differences were very visual.

Figure 5.13 presents the system behavior of a simple controller with no constraints. The controller is not bound to any price. Energy can be sold anytime and the sale is not bound to any price limit. The blue function denotes the power difference between the power production and the forecast. If the function is positive, excess energy is available,

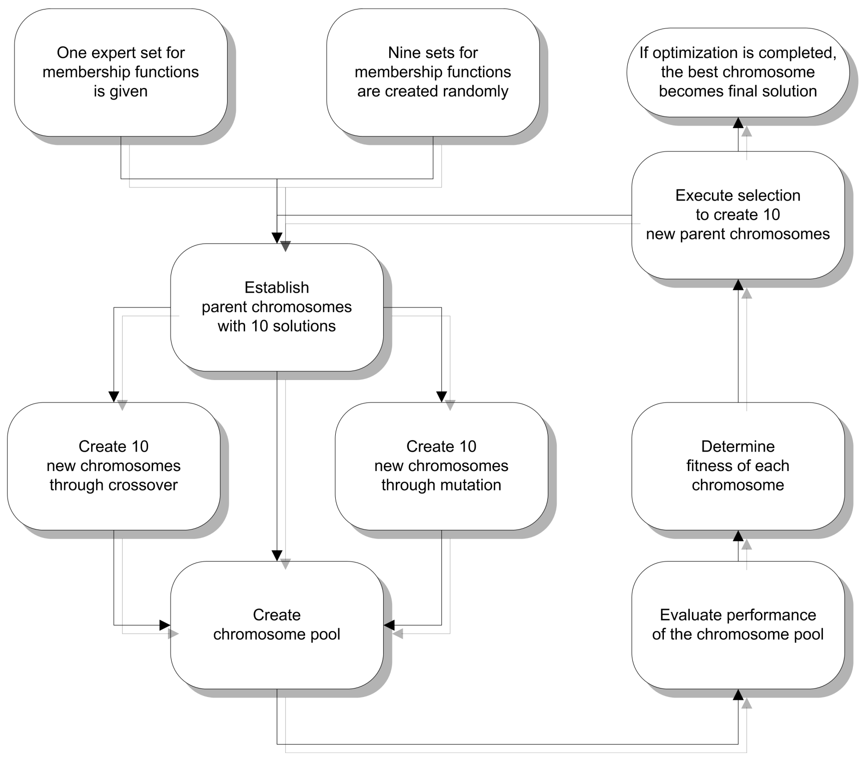

Figure 5.12: Flow Chart of the Optimization Procedure for the Fuzzy Logic Controller

which can be stored. If the function is negative, there is a power deficit, which needs to be offset. The black area underneath the power difference function indicates the power difference that existed after the energy storage stored or offset energy. Therefore, a white area symbolizes when energy was stored or offset. The green function represents the electricity price[1].

Figure 5.13 shows that energy is always sold when energy is needed and the power difference is negative. The revenue of this system is 18.0218.

Figure 5.14 shows a shift in sale of the energy. The system has the same underlying

[1]Since the price is limited and a reasonable normalization is possible, the electricity price was used as a price indicator.

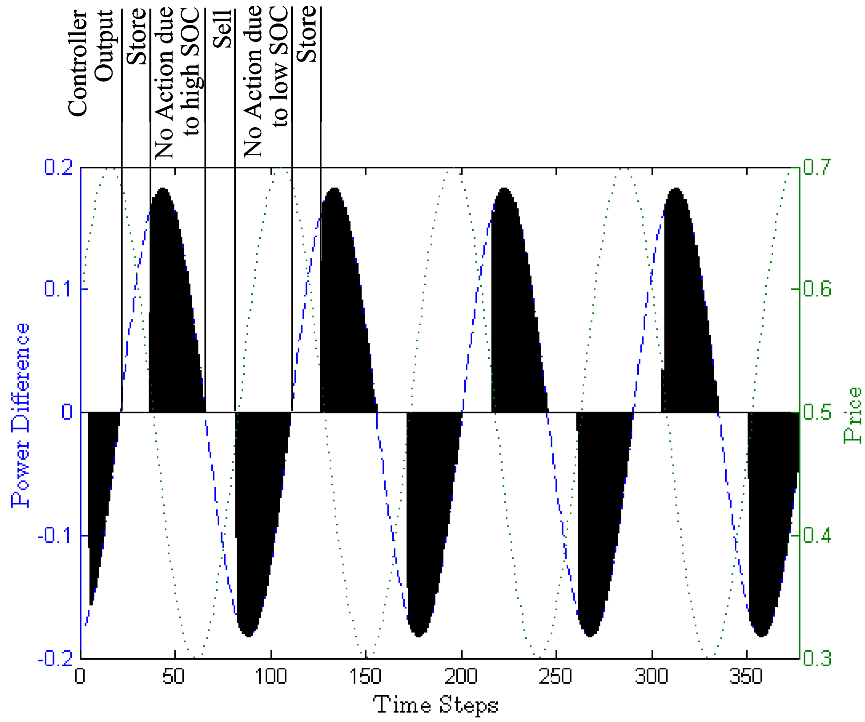

Figure 5.13: Sale Shift in the Test System with No Constraints

parameters as the earlier presented system; however, it is controlled by a optimized neural network controller. It is visible that the sales happened at a higher price, which led to a higher revenue (18.1708 points).

This test system shows that a better revenue can be achieved through a shift in the controls and that the neural network controller works as it was designed.

5.5 Summary

This Chapter presented the implementation of the biomimetic controllers and their specific modifications. It explained the general controller idea and the controller parameters.

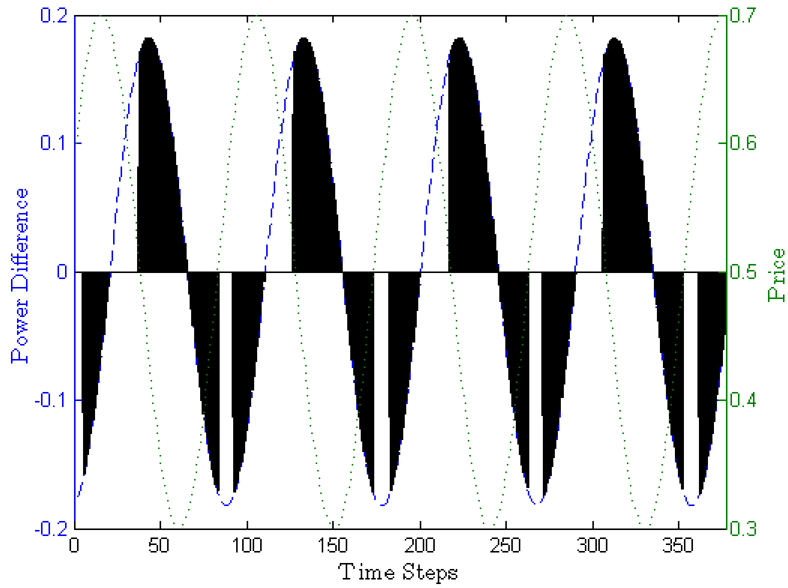

Figure 5.14: Sale Shift in the Test System by Neural Network Controller

For each important section, a test of each system was presented.

Chapter 6 – Simulation

6.1 General parameters

The final goal was to test the developed controller in a "simulated real-life" environment. Therefore, a power flow environment was programmed as a MatLab script. The environment calculated the power differences and relative price changes, and kept track of the battery's state of charge, as well as the energy provided to the grid. In addition, the environment (MatLab script called "EvaluateController.m") computed the cost function (as stated in Section 3.8) and provided feedback to the genetic algorithm during the optimization process. The simulation was based on real wind park power data and Mid-Columbia price data from April until mid December, 2008.

Even though the controller acted independent of the energy storage system, and the storage system could be represented by any stated technology in Section 1.1, in this simulation, parameters for the energy storage system were based on zinc/bromide battery technology. The main parameters are:

Efficiency The battery efficiency is 85% per half battery cycle [9].

Power Rating The power rating of the battery system is 0.2125 PU. This size is based on John Yen's master's thesis [35], in which he optimized the battery size based on the wind data from April to December 2008.

Capacity Rating The capacity rating is only a fourth of Yen's proposed rating (1.15 PU hr), because that size was based on a minimum of battery lifetime cycles. A system of that size would be cost intensive and could fill any given power difference. Shifting of the sale would not be necessary. Therefore, the capacity size was reduced to 0.2875 PU hr.

6.2 Simulation Scenarios

To determine the effectiveness of the controllers, a "reference model" was developed for comparison. The "reference model" is a simple controller that always provides power from the storage if the power difference is negative, and stores the energy if excess energy is available. For future reference, this model is called **"Simple Controller"**.

In addition to the simple controller, a **price constrained controller** was programmed. This controller is similar to the previous controller with the difference that energy is only provided from storage in times of a deficit, if the absolute price is above a certain dollar price. For the following test, the price minimum limit was set to $65.

In case of the biomimetic controllers, both were tested in their **initial and optimized versions**. One network weight set after the supervised training part became the initial neural network solution. The initial version for the fuzzy controller was based on one expert solution for the membership. Both controllers were optimized on a dataset of 1000 entries and later evaluated on a dataset with 40000 entries (each entry represents a period of 10 minutes with a total of 278 days).
The concept creates four further scenarios:

- Initial neural network controller
- Optimized neural network controller

- Initial fuzzy logic controller
- Optimized fuzzy logic controller

6.3 Simulation Results

The optimization results for both controllers are shown in Table 6.1, 6.2, and 6.3. The results were calculated based on the cost function stated in Section 3.8 and on 40000 data entries for the price and wind power data. Both biomimetic controllers were optimized on a dataset of 1000 entries over a period of 20 iterations. The pool of parent chromosomes and newly created chromosomes through mutation and cross-over had a size of ten chromosomes each. All results from the biomimetic controllers were based on an average of 5 or 10 test trials.

Table 6.1: Results for the Reference Model and Constrained Model

Simple	Cost-Based at $60
$12,553,810.60	$11,045,308.27

Table 6.2: Results for the Neural Network Controller

ANN Not Optimized	ANN Optimized
$10,896,371.00	$12,554,789.50

Table 6.3: Results for the Fuzzy Logic Controller

Fuzzy Not Optimized	Fuzzy Optimized
$10,952,000.43	$11,126,576.61

Results include the revenue from the entire energy sale over a course of 40000 time steps, including all penalties. It is important to note that the penalties on the total costs were at most one-fifth of the total revenue. The rest of the revenue originates from the electricity sale.

It is clearly visible that the simple controller performed better than the initial and optimized fuzzy controller. The initial neural network controller performs poorly as well; however, the optimization process changes the performance to a similar result as the simple controller. The revenue from a cost based controller is also below the reference controller.

6.4 Influence of the Optimization on the Results

Table 6.2 and 6.3 show that the optimization of a biomimetic controller leads to a better performance than the initial controller. While the improvements for the fuzzy controller were rather small (only 1.37%), the optimization of the neural network improved the performance by 14.8%. This difference could originate from "degrees of freedom" in which a chromosome was allowed to change. The membership function for one input parameter was only defined by one chromosome value. In addition, the mutation range of the fuzzy optimization was constrained to the limits of -1 and 1.

6.5 Influence of the Optimization Iterations on the Results

It was of interest if the results would change with a longer optimization period. Thus, the optimization was performed with 10, 20 , 50, and 100 iterations. Table 6.4 and 6.5 show the averaged simulation results.

Table 6.4: Results for the Neural Network Controller over Optimizations Trials with Different Lengths

Number of Iterations	Neural Net Initial	Neural Net Optimized
10	$11,045,308.27	$12,553,346.15
20	$10,896,371.00	$12,554,789.50
50	$10,903,349.89	$12,552,792.82
100	$10,898,863.45	$12,552,904.40

Table 6.5: Results for the Fuzzy Logic Controller over Optimizations Trials with Different Lengths

Number of Iterations	Fuzzy Initial	Fuzzy Optimized
10	$10,952,000.43	$11,097,405.65
20	$10,952,000.43	$11,126,576.61
50	$10,952,000.43	$11,065,756.10
100	$10,952,000.43	$11,116,524.95

The results of the initial fuzzy controller are constant, because they are based on the initial expert solution, which stays constant with every trial. The results show that the performance for each controller does not depend on the optimization length and does not change with a longer optimization; however, the neural network controller showed the best performance after 20 iterations. In this case, the neural network controller was slightly better than the simple controller, but not significantly so.

6.6 Visual Results of Optimization

Figure 6.1 to 6.6 show the results for each controller. The upper graphs always shows the power levels with the difference before (blue function) and after the energy storage system (blue bars). The price for each time step is represented by the green function. The white underneath the power difference function is important. If the area is white instead of blue, then the controller offset or stored energy in order to balance out the differences.

In the lower graph, the state-of-charge is presented. This graph is interesting because it shows when the battery is fully charged or empty. If the battery is full or empty and the current power difference trend continues, then the controller does not act until the power difference reverses.

Figure 6.3 and 6.4, as well as Figure 6.5 and 6.6 show the changes through the optimization process. For both controllers, the effects of the optimization are visible.

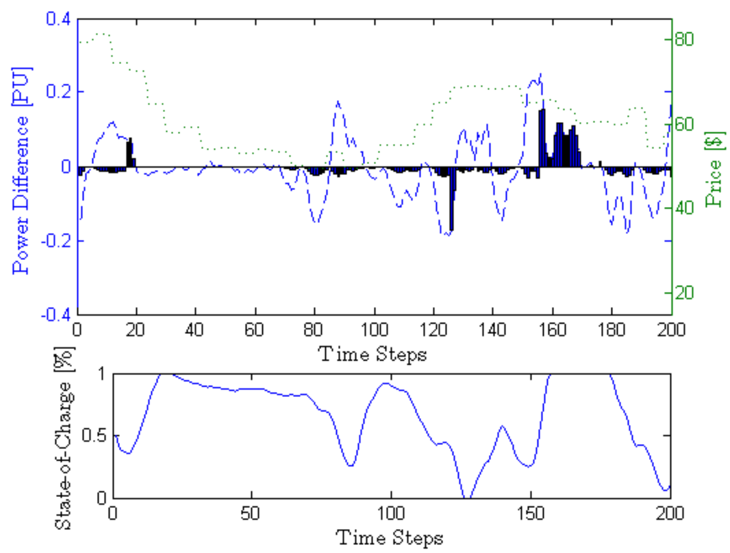

Figure 6.1: Visual Results of the Simple Controller over 200 Data Entries

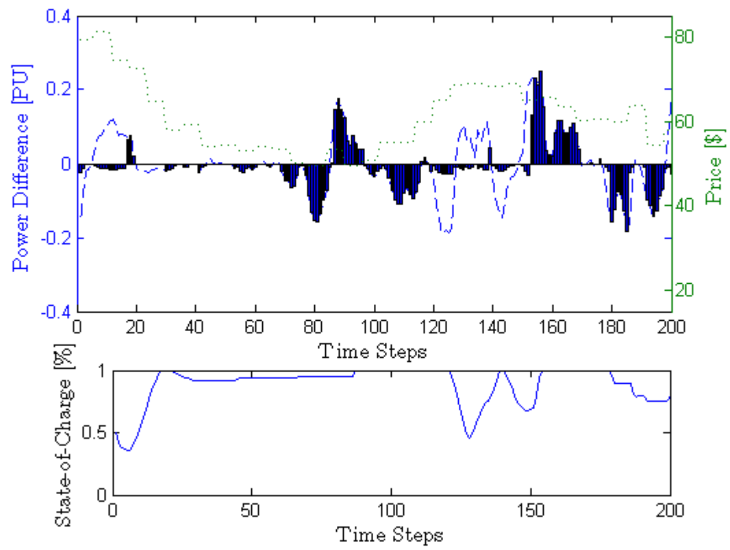

Figure 6.2: Visual Results of the Constrained Controller with a Price Limit at $60 over 200 Data Entries

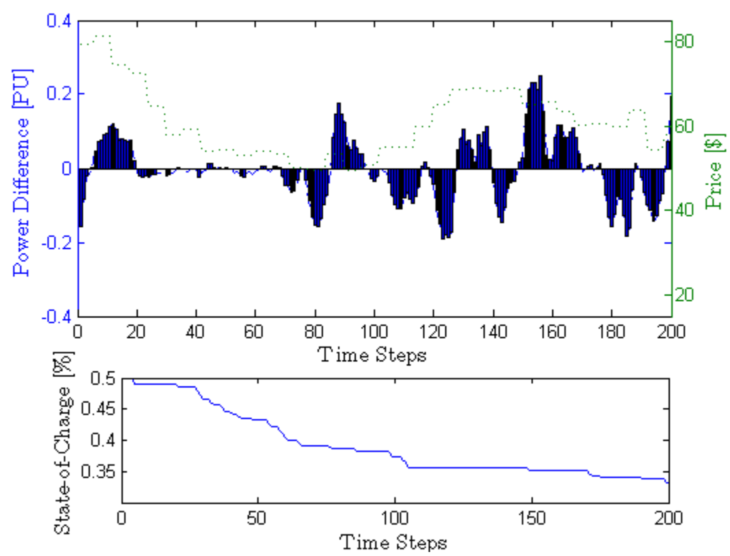

Figure 6.3: Visual Results of the Inital Neural Network Controller over 200 Data Entries

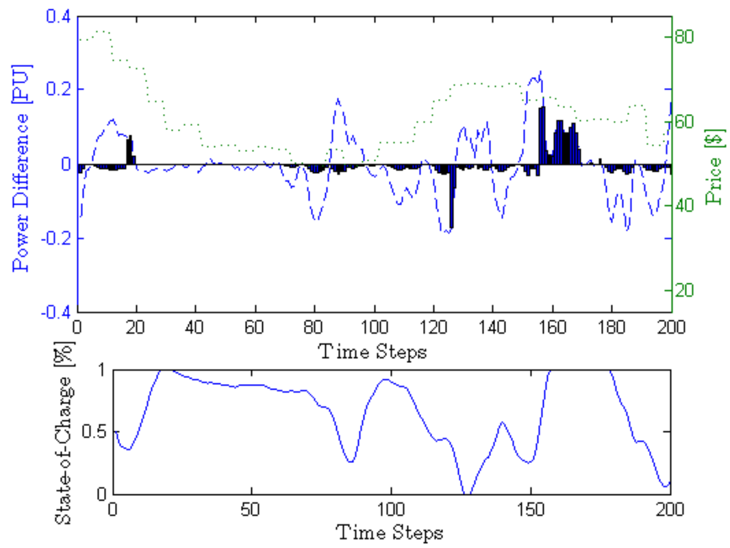

Figure 6.4: Visual Results of the Optimized Neural Network Controller over 200 Data Entries

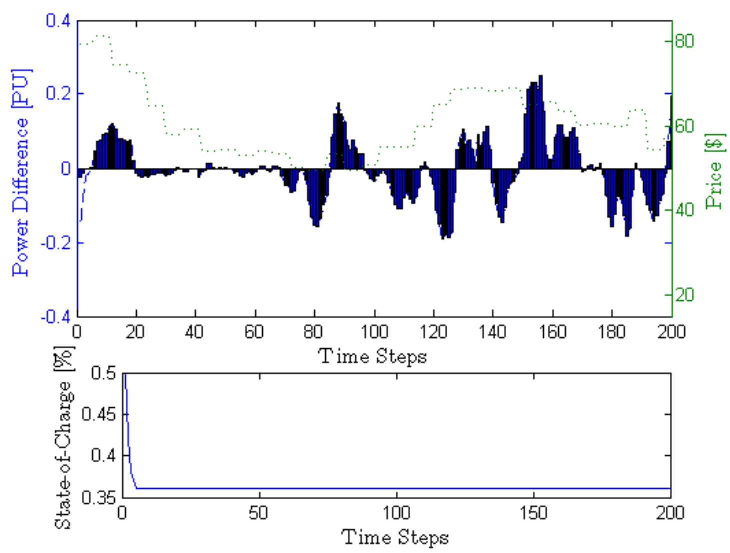

Figure 6.5: Visual Results of the Inital Fuzzy Logic Network Controller over 200 Data Entries

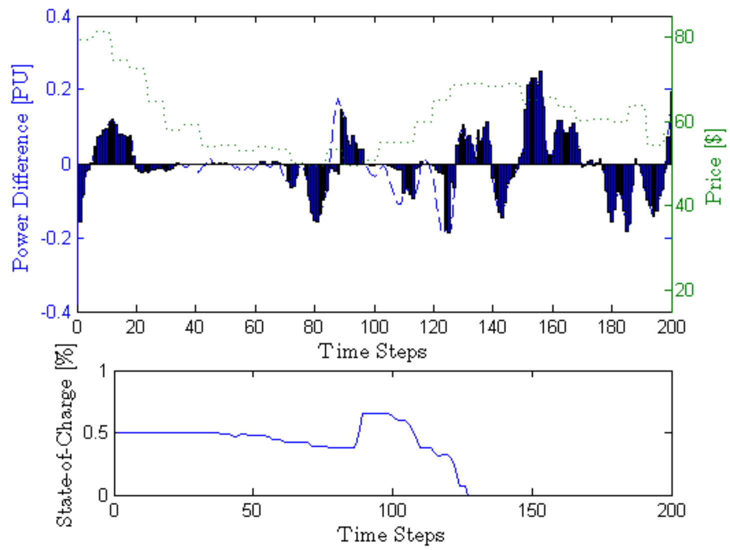

Figure 6.6: Visual Results of the Optimized Fuzzy Logic Controller over 200 Data Entries

6.7 Cost Function Including External Costs

It was also of interest to investigate how the cost function would change if the external costs, depending on the volume of saved CO_2, were considered. The presented cost functions from Section 3.8 were extended by the monetary value of saved CO_2, which is currently traded with roughly \$11.50 per ton of CO_2 [77]. In addition, the wind turbine manufacturer, Vestas, states in their environmental report [51] that one MWh produced by a wind turbine saves 0.82 ton of CO_2 emitted by conventional power generation sources.

Therefore, the external costs which can be saved were:

$$C_{Carbon} = E_{Produced} \times 0.82 tons\ CO_2/MWh \times \$11.50$$

The cost functions were then extended by C_{Carbon}. For each produced megawatt-hour by a wind turbine, the operator gains an additional amount, whereby the operator has to pay an additional environmental penalty if the forecast is not met and the energy has to be produced by a conventional source like a gas turbine. In the case of under forecasting, the operator gains no benefit of the external costs, because the volume could not have been sold at the CO_2 market beforehand:

$$\begin{aligned} J(t) &= P_F \times [C(t) + C_{Carbon}] \\ &+ (P_G - P_F) \times 0.9 \times C_{under\ forecasting} \end{aligned}$$

If the electricity generation is below the prediction:

$$\begin{aligned} J(t) &= P_F \times [C(t) + C_{Carbon}] \\ &- (P_F - P_G) \times 1.1 \times C_{over\ forecasting} \times C_{Carbon} \end{aligned}$$

The results of this cost function are stated in Table 6.6, 6.7, and 6.8.

Table 6.6: Results for the Reference Model and Constrained Model with External Costs

Simple	Cost-Based at \$60
\$15,055,568.14	\$13,294,369.36

Table 6.7: Results for the Neural Network Controller with External Costs

ANN Not Optimized	ANN Optimized
\$13,136,244.42	\$15,055,345.31

Table 6.8: Results for the Fuzzy Logic Controller with External Costs

Fuzzy Not Optimized	Fuzzy Optimized
\$13,195,669.90	\$13,399,693.87

It turns out that the cost function with external costs does not change the order of the controller performance, it simply adds an additional amount to the results of the cost function.

Chapter 7 – Conclusion

This thesis presented the development of biomimetic control strategies for the optimal use of renewable sources and energy storage technologies. Two controller types were presented in Chapter 6, a neural network and a fuzzy logic controller, which were optimized by a genetic algorithm. Both controllers were tested on 40000 data samples.

As the results show, optimized biomimetic control strategies can adapt to unknown environments through changing either the neural network weights or the membership functions. However, the performance of both controllers did not exceed the simple controller, for various reasons.

After all tests, it is believed that the main reason for the under-performance of the controller is not the controller itself, but the price forecasting method. Each controller was envisioned to make a power split decision based on the relationship between a current price and a future price. If the price rises in the future, then it makes more sense to sell the stored electricity later to increase the profit. However, the used price forecasting method, the persistence model, does not predict a trend, since the future value is the same as the current value. This fact limits the significance of the future price behavior. In addition, it also explains the difference in controller behaviors between the neural network and the fuzzy logic controller. The fuzzy controller is based on fixed rules to determine the controller output; thus, the controller behavior was limited. For example, the input case “current rel. price change LOW” with “future rel. price change HIGH” should have caused the controller to store energy. However, the rule was never applied.

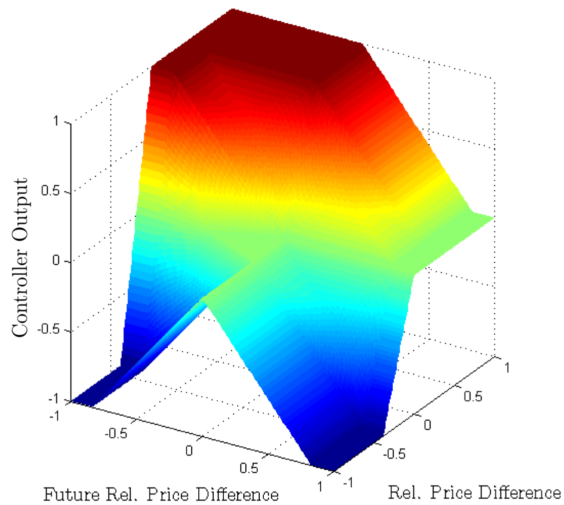

(a) Surface Plot

(b) Contour Plot

Figure 7.1: Visualization of the Fuzzy Logic Controller Output for Different Price Input and at Fixed SOC (Low = -1) and Power Difference (High Positive = 1)

Figures 7.1 (a) and (b) show the fuzzy controller output for variable current and future price inputs at a constant, low SOC and constant positive power difference. Figure (a) presents well that, for a high current price with a falling trend in the future, all available energy of the storage system should have sold (a sale is represented by a positive value and the storage action is represented by a negative value). However, this controller output was never reached because all solutions could only be obtained from the area around the solid, black line in Figure 7.1 (b), in which is current price is the same as the future price (based on the persistence model).

This failure in the structure demonstrated the power of an optimized neural network controller; During the optimization, the network weights were adapted in order to increase the revenue. Since both price values were the same, the significance within the network was reduced by lower weights. Only the battery state-of-charge and the power difference were of influence in the optimized network. These two parameters have the same influences on the behavior of the simple controller, which explains why the neural network controller could never out perform the simple controller. However, the values between the simple and the neural network controller were very similar.

7.1 Future Work

Based on the work with biomimetic control theory, it is of interest to test the same controller types with commercial price forecast data, which presents a trend in the price behavior. It would be interesting, if the performance of the controller finally out-performs the simple controller.

If a model of the price behavior can be determined, the controller could also be modeled with an estimator. However, a model for this behavior might not exist. Otherwise prices could be estimated and the market could be manipulated.

With the rising importance of distributed generation in power systems, it will be of immense interest to investigate further biomimetic control techniques like multi-agent systems (MAS). In a multi-agent system, entities (generation, load, etc.) are modeled as agents, which communicate with each other. This concept could be applied to the energy power split decision, where the storage unit, the wind park, the grid, etc. are all modeled as individual agents. The control of each entity is done locally, and not by a central controller. This concept is extremely powerful if multiple wind parks have access to multiple storage units. The idea of MAS in power systems is already tested for distributed generation project for PV generators [81].

Bibliography

[1] Energy Information Administration, "International energy statistics," May 2009. [Online]. Available: http://www.eia.doe.gov/

[2] P. Hawken, A. Lovins, and H. Lovins, *Natural Capitalism: Creating the Next Industrial Revolution*. Little Brown & Company, October 2000. [Online]. Available: http://www.natcap.org

[3] G. Boyle, *Renewable electricity and the grid*. Earthscan, 2007.

[4] North American Electric Reliability Corporation, "Accommodating high levels of variable generation," Tech. Rep., April 2009. [Online]. Available: http://www.nerc.com/files/IVGTF_Report_041609.pdf

[5] R. Dell, "Energy storage a key technology for global energy sustainability," *Journal of Power Sources*, vol. 100, no. 1-2, pp. 2–17, November 2001. [Online]. Available: http://dx.doi.org/10.1016/S0378-7753(01)00894-1

[6] W. Leonhard and E. M. Grobe, "Sustainable electrical energy supply with wind and pumped storage - a realistic long-term strategy or utopia?" in *Power Engineering Society General Meeting, 2004. IEEE*, 2004, pp. 1221–1225 Vol.2. [Online]. Available: http://dx.doi.org/10.1109/PES.2004.1373049

[7] J. Mcdowall, "Integrating energy storage with wind power in weak electricity grids," *Journal of Power Sources*, vol. 162, no. 2, pp. 959–964, November 2006. [Online]. Available: http://dx.doi.org/10.1016/j.jpowsour.2005.06.034

[8] J. W. Tester, E. M. Drake, M. J. Driscoll, M. W. Golay, and W. A. Peters, *Sustainable energy*. MIT Press, 2005.

[9] S. M. Schoenung and W. V. Hassenzahl, "Long- vs. short-term energy storagetechnologies analysis - a life-cycle cost study," Sandia National Laboratories, Tech. Rep., August 2003.

[10] S. Kalogirou, Ed., *Artificial intelligence in energy and renewable energy systems*. Nova Science, 2006.

[11] K. Warwick, A. Ekwue, and R. Aggarwal, *Artificial intelligence techniques in power systems*, ser. IEE Power Engineering Series. The Institution of Electrical Engineers, 1997, vol. 22.

[12] H. Yan and P. B. Luh, "A fuzzy optimization-based method for integrated power system scheduling and inter-utility power transaction with uncertainties," *Power Systems, IEEE Transactions on*, vol. 12, no. 2, pp. 756–763, 1997. [Online]. Available: http://dx.doi.org/10.1109/59.589672

[13] F. Jurado, "Neuro-fuzzy control for autonomous winddiesel systems using biomass," *Renewable Energy*, vol. 27, no. 1, pp. 39–56, September 2002. [Online]. Available: http://dx.doi.org/10.1016/S0960-1481(01)00170-7

[14] P. S. Panickar, M. S. Rahman, and S. M. Islam, "A neuro-fuzzy model for the control operation of a wind-diesel-battery hybrid power system," *JOURNAL OF ELECTRICAL AND ELECTRONICS ENGINEERING AUSTRALIA*, 2002. [Online]. Available: http://www.itee.uq.edu.au/~{}aupec/aupec01/060_PANICKAR_AUPEC01paper%20revised.pdf

[15] P. Attaviriyanupap, H. Kita, E. Tanaka, and J. Hasegawa, "A fuzzy-optimization approach to dynamic economic dispatch considering uncertainties," *Power Systems, IEEE Transactions on*, vol. 19, no. 3, pp. 1299–1307, 2004. [Online]. Available: http://dx.doi.org/10.1109/TPWRS.2004.831272

[16] V. Miranda and P. S. Hang, "Economic dispatch model with fuzzy wind constraints and attitudes of dispatchers," *Power Systems, IEEE Transactions on*, vol. 20, no. 4, pp. 2143–2145, 2005. [Online]. Available: http://dx.doi.org/10.1109/TPWRS.2005.857930

[17] R. Rojas, *Theorie der neuronalen Netze*. Springer, 1993. [Online]. Available: http://page.mi.fu-berlin.de/rojas/neural/

[18] K. M. Passino and S. Yurkovich, *Fuzzy Control*. Addison-Wesley, 1998. [Online]. Available: http://www.ece.osu.edu/~{}passino/FCbook.pdf

[19] D. B. Fogel, T. Bäck, and Z. Michalewicz, *Evolutionary Computation: Basic algorithms and operators*. CRC Press, 2000. [Online]. Available: http://books.google.com/books?id=4HMYCq9US78C

[20] K. M. Passino, *Biomimicry for optimization, control, and automation*. Springer, 2004.

[21] S. Zak, *Systems and Control*. Oxford University Press, 2003.

[22] S. D. Sudhoff, "Evolutionary design of pmsm machines," May 2009.

[23] K. Tumer, "Neural network basics," Corvallis, OR, October 2008.

[24] R. O. Duda, P. E. Hart, and D. G. Stork, *Pattern Classification*, D. G. Stork, Ed. Wiley, 2007.

[25] C. W. Bary, *Operational Economics of Electric Utilities.* Columbia University Press, 1963.

[26] S. Mathew, *Wind Energy and Environment.* Heidelberg, Germany: Springer, 2005, ch. 6, pp. 179–207.

[27] M. Robinson, "An overview of the midwest iso market design," March 2009. [Online]. Available: http://www.ece.umn.edu/groups/power/monthsem/pres_robinson.pdf

[28] H. Khatib, *Economic evaluation of projects in the electricity supply industry*, ser. IEE Power & Energy Series. Institution of Electrical Engineers, 2003.

[29] European Energy Exchange, "Eex intraday-energy-trading," May 2009. [Online]. Available: http://www.eex.com/en/Download/Market%20Data

[30] NYMEX, "Nymex dow jones mid-columbia electricity index futures," 2008. [Online]. Available: http://www.nymex.com/DO_desc.aspx

[31] T. Ackermann, J. R. Abbad, I. M. Dudurych, I. Erlich, H. Holttinen, J. R. Kristoffersen, and P. E. Sorensen, "European balancing act," *IEEE power & energy magazine*, December 2007. [Online]. Available: http://www.awea.org/utility/pdf/04383127Europe.pdf

[32] L. Dale, "Total cost estimates for large-scale wind scenarios in uk," *Energy Policy*, vol. 32, no. 17, pp. 1949–1956, November 2004. [Online]. Available: http://dx.doi.org/10.1016/j.enpol.2004.03.012

[33] A. E. Ingram, "Storage options and sizing for utility scale integration of wind energy plants," *Proceedings of ISEC2005*, August 2005.

[34] T. Wizelius, *Developing wind power projects.* London, UK: Earthscan, 2007.

[35] J. Yen, "Analysis and optimal sizing for an energy storage system for wind farm applications," Master's thesis, Oregon State University, June 2009.

[36] M. Milligan, M. Schwartz, and Y. Wan, "Statistical wind power forecasting models: Results foru.s. wind farms," in *WINDPOWER 2003.* Golden, CO: National Renewable Energy Laboratory, May 2003. [Online]. Available: http://www.nrel.gov/docs/fy03osti/33956.pdf

[37] Y.-H. Song and X.-F. Wang, *Operation of market-oriented power systems*, ser. Power Systems, Y.-H. Song, Ed. Springer, 2003.

[38] A. Sfetsos, "A comparison of various forecasting techniques applied to mean hourly wind speed time series," *Renewable Energy*, vol. 21, no. 1, pp. 23–35, September 2000. [Online]. Available: http://dx.doi.org/10.1016/S0960-1481(99)00125-1

[39] A. More, "Forecasting wind with neural networks," *Marine Structures*, vol. 16, no. 1, pp. 35–49, February 2003. [Online]. Available: http://dx.doi.org/10.1016/S0951-8339(02)00053-9

[40] F. Consoli, D. Allen, I. Boustead, J. Fava, and F. Franklin, *Guidelines for life-cycle assessment: a" Code of Practice"*. Society of Environmental Toxicology and Chemistry, 1993.

[41] I. S. Organization, "Iso 14040:2006 - environmental management - life cycle assessment - principles and framework," International Organization for Standardization, Tech. Rep., 2006. [Online]. Available: http://www.iso.org/iso/catalogue_detail?csnumber=37456

[42] C. T. Hendrickson, L. B. Lave, and S. Matthews, *Life cycle controversies*. Resources for the Future, 2006, ch. 1, pp. 5–6. [Online]. Available: http://books.google.com/books?id=-w2KtGXa-OAC

[43] S. New, "A critical appraisal of aspects of the lean chain approach," *European Journal of Purchasing & Supply Management*, vol. 3, no. 2, pp. 93–102, June 1997. [Online]. Available: http://dx.doi.org/10.1016/S0969-7012(96)00019-6

[44] Vestas A/S, "Life cycle assessment (lca)," May 2009. [Online]. Available: http://www.vestas.com/en/about-vestas/sustainability/wind-turbines-and-the-environment/life-cycle-assessment-(lca).aspx

[45] L. Schleisner, "Life cycle assessment of a wind farm and related externalities," *Renewable Energy*, vol. 20, pp. 279–288, 2000.

[46] N. Jungbluth, C. Bauer, R. Dones, and R. Frischknecht, "Life cycle assessment for emerging technologies: Case studies for photovoltaic and wind power," *The International Journal of Life Cycle Assessment*, vol. 10, no. 1, pp. 24–34, January 2005. [Online]. Available: http://dx.doi.org/10.1065/lca2004.11.181.3

[47] J. Weinzettel, M. Reenaas, C. Solli, and E. Hertwich, "Life cycle assessment of a floating offshore wind turbine," *Renewable Energy*, vol. 34, no. 3, pp. 742–747, March 2009. [Online]. Available: http://dx.doi.org/10.1016/j.renene.2008.04.004

[48] E. Martinez, F. Sanz, S. Pellegrini, E. Jimenez, and J. Blanco, "Life cycle assessment of a multi-megawatt wind turbine," *Renewable Energy*, vol. 34, no. 3, pp. 667–673, March 2009. [Online]. Available: http://dx.doi.org/10.1016/j.renene.2008.05.020

[49] M. Pehnt, "Dynamic life cycle assessment (lca) of renewable energy technologies," *Renewable Energy*, vol. 31, no. 1, pp. 55–71, January 2006. [Online]. Available: http://dx.doi.org/10.1016/j.renene.2005.03.002

[50] Vestas A/S, "Life cycle assessment of electricity produced from onshore sited wind power plants based on vestas turbines," Vestas A/S, Tech. Rep., December 2006.

[51] Vestas A/S, "Vestas lifecycle assessment of a vestas onshore wind turbine," Vestas A/S, Tech. Rep., 2008.

[52] Vestas A/S, "Putting numbers on green performance," *Vestas Wind*, vol. 15, February 2009. [Online]. Available: http://nozebra.ipapercms.dk/Vestas/VestasWind/UK/1509/

[53] M. Lenzen, "Wind turbines in brazil and germany: an example of geographical variability in life-cycle assessment," *Applied Energy*, vol. 77, no. 2, pp. 119–130, February 2004. [Online]. Available: http://dx.doi.org/10.1016/S0306-2619(03)00105-3

[54] M. Goedkoop, A. De Schryver, and M. Oele, *SimaPro 7 - Introduction into LCA*. Amersfoort, The Netherlands: PRé Consultants, February 2008.

[55] A. A. Jensen, L. Hoffman, B. T. Moller, and A. Schmidt, "Life cycle assessment - a guide to approaches, experiences and information sources," August 1997.

[56] "Simapro 7 software," http://www.pre.nl/simapro.

[57] L. Dreyer, A. Niemann, and M. Hauschild, "Comparison of three different lcia methods: Edip97, cml2001 and eco-indicator 99," *The International Journal of Life Cycle Assessment*, vol. 8, no. 4, pp. 191–200, July 2003. [Online]. Available: http://dx.doi.org/10.1007/BF02978471

[58] H. Wenzel, M. Hauschild, and L. Alting, *Environmental Assessment of Products*. Springer, 2000. [Online]. Available: http://books.google.com/books?id=fpKprrwMQ0kC

[59] J. B. Guinée, *LCA - An operational guide to the ISO-standards*. Universiteit Leiden, May 2001. [Online]. Available: http://cml.leiden.edu/research/industrialecology/researchprojects/finished/new-dutch-lca-guide

[60] M. Goedkoop and R. Spriensma, *The Eco-indicator 99: A damage oriented method for life cycle impact assessment*. PRé, 2000. [Online]. Available: http://www.pre.nl/download/EI99_Manual.pdf

[61] K. R. Haapala, J. L. Rivera, and J. W. Sutherland, "Application of life cycle assessment methods to sustainable product design and manufacturing," *International Journal of Innovative Computing, Information and Control*, vol. 4, no. 3, pp. 577–591, March 2008.

[62] P. Consultants, "Eco-indicator 99: Acknowledgements," 2009. [Online]. Available: http://www.pre.nl/eco-indicator99/acknowledgements.htm

[63] R. Frischknecht, N. Jungbluth, H. Althaus, G. Doka, R. Dones, S. Hellweg, R. Hischier, S. Humbert, M. Margni, T. Nemecek, and M. Spielmann, "Implementation of life cycle impact assessment methods," Swiss Centre for Life Cycle Inventories, Tech. Rep., 2007.

[64] Vestas A/S, "Environmental statement 2008 - vestas blades, isle of white, england," Vestas A/S, Tech. Rep., February 2009. [Online]. Available: http://www.vestas.com/Files%2FFiler%2FEN%2FSustainability%2FSite_descriptions%2F2008%2FVES_BLA_IsleWight_England.pdf

[65] P. J. Tavner, J. Xiang, and F. Spinato, "Reliability analysis for wind turbines," *Wind Energy*, vol. 10, no. 1, pp. 1–18, July 2006. [Online]. Available: http://doi.wiley.com/10.1002/we.204

[66] G. J. W. van Bussel and M. B. Zaaijer, "Reliability, availability and maintenance aspects of large-scale offshore wind farms, a concepts study," in *Proceedings of MAREC*. Delft University of Technology, 2001. [Online]. Available: http://www.ecn.nl/docs/dowec/2001-MAREC-RAMS.pdf

[67] B. P. Mcniff, W. D. Musial, and R. Errichello, "Variations in gear fatigue life for different wind turbine braking strategies," in *A WEA Wind Power '90*, September 1990.

[68] E. Echavarria, B. Hahn, G. J. W. van Bussel, and T. Tomiyama, "Reliability of wind turbine technology through time," *Journal of Solar Energy Engineering*, vol. 130, no. 3, pp. 031 005+, 2008. [Online]. Available: http://dx.doi.org/10.1115/1.2936235

[69] UNFCCC, "Clean development mechanism," United Nations Framework Convention on Climate Change, May 2009. [Online]. Available: http://cdm.unfccc.int/about/index.html

[70] TFS Green, "Joint implementation (ji) introduction," 2009. [Online]. Available: http://www.tfsgreen.com/global-markets/joint-implementation/

[71] European Commission, "Emission trading system (eu ets)," european Parliament, May 2009. [Online]. Available: http://ec.europa.eu/environment/climat/emission/index_en.htm

[72] Environmental Protection Agency, "Cap and trade," April 2009. [Online]. Available: http://www.epa.gov/captrade/

[73] H. A. Waxman, "Clean energy bill," U.S. House of Representatives. [Online]. Available: http://energycommerce.house.gov/Press_111/20090331/acesa_discussiondraft.pdf

[74] B. Cain, "Oregon governor makes pitch for cap-and-trade," May 2009. [Online]. Available: http://www.theworldlink.com/articles/2009/02/06/news/doc498c7f8b730fd174395361.txt

[75] Carbon Tax Center, "What's a carbon tax?" February 2009. [Online]. Available: http://www.carbontax.org/introduction

[76] Carbon Tax Center, "Carbon tax vs. cap-trade," Carbon Tax Center, New York, NY, May 2009. [Online]. Available: http://www.carbontax.org/issues/carbon-taxes-vs-cap-and-trade/

[77] European Energy Exchange, "Carbix trading information," May 2009. [Online]. Available: http://www.eex.com/de/Downloads/Marktdaten

[78] U.S. Environmental Protection Agency, "Epa proposes new regulations for the national renewable fuel standard program for 2010 and beyond," U.S. Environmental Protection Agency, http://www.epa.gov, May 2009. [Online]. Available: http://www.epa.gov/OMS/renewablefuels/420f09023.htm

[79] Y. Makarov, S. Lu, B. Mcmanus, and J. Pease, "The future impact of wind on bpa power system ancillary services," in *Transmission and Distribution Conference and Exposition*, IEEE/PES. IEEE/PES, April 2008.

[80] S. Theodoridis and K. Koutroumbas, *Pattern recognition*. Academic Press, 2006. [Online]. Available: http://books.google.com/books?id=gAGRCmp8Sp8C

[81] J. Lagorse, D. Paire, and A. Miraoui, "A multi-agent system for energy management of distributed power sources," *Renewable Energy*, April 2009. [Online]. Available: http://dx.doi.org/10.1016/j.renene.2009.02.029

APPENDICES

Table 1: Detailed Life Cycle Assessment Inventory

Component	SimaPro Material Information	Weight in tons	Note
Foundation		**832**	
	Concrete (reinforced) I	832	
Tower		**135.2**	
	Steel ETH S	126.1	
	Copper ETH S	1.3	
	ABS I	2	
	Aluminium 0% recycled ETH S	0.26	Vestas uses Alumminium 90% recycled
	Aluminium 100% recycled ETH S	2.34	
	Electronics for control units/RER S	2.2	
	Lubricating oil, at plant/RER S	1	
Nacelle Shell		**24.2**	
	Glass fibre reinforced plastic	1.8	
	Electro steel ETH S	13	
	X5CrNi18 (304) I	7.8	Counts for stainless steel
	ABS I	1	
	Electronics for control units/RER S	0.3	
	Lubricating oil, at plant/RER S	0.3	
Gearbox		**15.25**	
	Cast iron ETH S	11.8	
	Steel ETH S	3.45	

Continued on Next Page...

Table 1 – Continued

Component	SimaPro Material Information	Weight in tons	Note
Generator		**9.09**	
	Cast iron ETH S	6.23	
	Steel ETH S	1.83	
	Copper ETH S	1.03	
Blade		**7.40**	
	Birch I	4.17	Includes Balsa wood
	Epoxy resin I	2.34	
	Glass fibre reinforced plastic	0.89	
Hub/Spinner		**20**	
	Cast iron ETH S	11.3	
	Electro steel ETH S	1.5	
	Steel ETH S	4.2	
	Epoxy resin I	2.173	
	Glass fibre reinforced plastic	0.827	
Int. cables		**0.8218**	
	Copper ETH S	0.17	
	ABS I	0.303	
	Aluminium 0% recycled ETH S	0.0348	Vestas uses Alumminium 90% recycled
	Aluminium 100% recycled ETH S	0.314	
Transformer		**3.091**	
	Steel ETH S	1.02	
	Copper ETH S	0.571	

Continued on Next Page...

Table 1 – Continued

Component	**SimaPro Material Information**	**Weight in tons**	**Note**
	Aluminium 0% recycled ETH S	0.05	Vestas uses Alumminium 90% recycled
	Aluminium 100% recycled ETH S	0.45	
	Epoxy resin I	1	

Table 2: Detailed Neural Network Training Set

Rules Number	**SOC**	**Power Difference**	**Rel. Price Difference**	**Future Price Rel. Difference**	**Controller Output**
1	Low	Energy Deficit	Low	Low	Store
2	Low	Energy Deficit	Low	High	Store
3	Low	Energy Deficit	High	Low	Sell
4	Low	Energy Deficit	High	High	Hold
5	Low	Energy Surplus	Low	Low	Sell
6	Low	Energy Surplus	Low	High	Store
7	Low	Energy Surplus	High	Low	Sell
8	Low	Energy Surplus	High	High	Hold
9	High	Energy Deficit	Low	Low	Sell
10	High	Energy Deficit	Low	High	Hold
11	High	Energy Deficit	High	Low	Sell
12	High	Energy Deficit	High	High	Hold
13	High	Energy Surplus	Low	Low	Sell
14	High	Energy Surplus	Low	High	Hold
15	High	Energy Surplus	High	Low	Sell
16	High	Energy Surplus	High	High	Sell

Table 3: Detailed Fuzzy Controller Rules

Rules Number	SOC	Power Difference	Rel. Price Difference	Future Price Rel. Difference	Controller Output
1	Low	Energy Surplus	Low	Low	*Store*
2	Low	Energy Surplus	Low	Medium	Store
3	Low	Energy Surplus	Low	High	*Store*
4	Low	Energy Surplus	Medium	Low	Hold
5	Low	Energy Surplus	Medium	Medium	Hold
6	Low	Energy Surplus	Medium	High	Store
7	Low	Energy Surplus	High	Low	*Sell*
8	Low	Energy Surplus	High	Medium	Hold
9	Low	Energy Surplus	High	High	*Hold*
10	Low	No Deficit/Surplus	Low	Low	Hold
11	Low	No Deficit/Surplus	Low	Medium	Store
12	Low	No Deficit/Surplus	Low	High	Store
13	Low	No Deficit/Surplus	Medium	Low	Sell
14	Low	No Deficit/Surplus	Medium	Medium	Hold
15	Low	No Deficit/Surplus	Medium	High	Store
16	Low	No Deficit/Surplus	High	Low	Sell
17	Low	No Deficit/Surplus	High	Medium	Sell
18	Low	No Deficit/Surplus	High	High	Hold
19	Low	Energy Deficit	Low	Low	*Store*
20	Low	Energy Deficit	Low	Medium	Hold

Continued on Next Page...

Table 3 – Continued

Rules Number	**SOC**	**Power Difference**	**Rel. Price Difference**	**Future Rel. Price Difference**	**Controller Output**
21	Low	Energy Deficit	Low	High	*Store*
22	Low	Energy Deficit	Medium	Low	Sell
23	Low	Energy Deficit	Medium	Medium	Hold
24	Low	Energy Deficit	Medium	High	Hold
25	Low	Energy Deficit	High	Low	*Sell*
26	Low	Energy Deficit	High	Medium	Sell
27	Low	Energy Deficit	High	High	*Hold*
28	Medium	Energy Surplus	Low	Low	Hold
29	Medium	Energy Surplus	Low	Medium	Store
30	Medium	Energy Surplus	Low	High	Store
31	Medium	Energy Surplus	Medium	Low	Sell
32	Medium	Energy Surplus	Medium	Medium	Hold
33	Medium	Energy Surplus	Medium	High	Store
34	Medium	Energy Surplus	High	Low	Sell
35	Medium	Energy Surplus	High	Medium	Sell
36	Medium	Energy Surplus	High	High	Hold
37	Medium	No Deficit/Surplus	Low	Low	Hold
38	Medium	No Deficit/Surplus	Low	Medium	Hold
39	Medium	No Deficit/Surplus	Low	High	Hold
40	Medium	No Deficit/Surplus	Medium	Low	Sell
41	Medium	No Deficit/Surplus	Medium	Medium	Hold
42	Medium	No Deficit/Surplus	Medium	High	Hold

Continued on Next Page…

Table 3 – Continued

Rules Number	**SOC**	**Power Difference**	**Rel. Price Difference**	**Future Rel. Price Difference**	**Controller Output**
43	Medium	No Deficit/Surplus	High	Low	Sell
44	Medium	No Deficit/Surplus	High	Medium	Sell
45	Medium	No Deficit/Surplus	High	High	Hold
46	Medium	Energy Deficit	Low	Low	Hold
47	Medium	Energy Deficit	Low	Medium	Hold
48	Medium	Energy Deficit	Low	High	Store
49	Medium	Energy Deficit	Medium	Low	Store
50	Medium	Energy Deficit	Medium	Medium	Hold
51	Medium	Energy Deficit	Medium	High	Hold
52	Medium	Energy Deficit	High	Low	Sell
53	Medium	Energy Deficit	High	Medium	Sell
54	Medium	Energy Deficit	High	High	Hold
55	High	Energy Surplus	Low	Low	*Sell*
56	High	Energy Surplus	Low	Medium	Store
57	High	Energy Surplus	Low	High	*Hold*
58	High	Energy Surplus	Medium	Low	Sell
59	High	Energy Surplus	Medium	Medium	Store
60	High	Energy Surplus	Medium	High	Store
61	High	Energy Surplus	High	Low	*Sell*
62	High	Energy Surplus	High	Medium	Sell
63	High	Energy Surplus	High	High	*Hold*

Continued on Next Page…

Table 3 – Continued

Rules Number	**SOC**	**Power Difference**	**Rel. Price Difference**	**Future Rel. Price Difference**	**Controller Output**
64	High	No Deficit/Surplus	Low	Low	*Hold*
65	High	No Deficit/Surplus	Low	Medium	Hold
66	High	No Deficit/Surplus	Low	High	*Hold*
67	High	No Deficit/Surplus	Medium	Low	Sell
68	High	No Deficit/Surplus	Medium	Medium	*Hold*
69	High	No Deficit/Surplus	Medium	High	Hold
70	High	No Deficit/Surplus	High	Low	*Sell*
71	High	No Deficit/Surplus	High	Medium	Sell
72	High	No Deficit/Surplus	High	High	*Sell*
73	High	Energy Deficit	Low	Low	*Sell*
74	High	Energy Deficit	Low	Medium	Sell
75	High	Energy Deficit	Low	High	*Hold*
76	High	Energy Deficit	Medium	Low	Sell
77	High	Energy Deficit	Medium	Medium	Sell
78	High	Energy Deficit	Medium	High	Sell
79	High	Energy Deficit	High	Low	*Sell*
80	High	Energy Deficit	High	Medium	Sell
81	High	Energy Deficit	High	High	*Sell*